Arabian Journal of Geosciences (2020) 13: 1106
https://doi.org/10.1007/s12517-020-05979-3

REVIEW PAPER

Fan morphology evidence on Late Quaternary deformation in the southern front of the Central and Eastern Alborz Mountains in the Eyvanekey, Garmsar, Semnan areas, Northern Iran

Soheila Bouzari[1]

Received: 29 August 2019 / Accepted: 3 September 2020 / Published online: 17 October 2020

Abstract
Although numerous studies have been done on the Alborz Mountains, few have examined Quaternary events based on alluvial fans which are located in front of the southern limb of the Central and Eastern Alborz Mountains. This study analyzed the morphometric indexes for 131 alluvial fans (three generations) in the Eyvanekey, Garmsar, and Semnan areas (A_s, WLF, Bull, F_a, F_s, F_g, F_c, R) as well as for basins (D_a, AF, T, B_s), mountain fronts (Fmf, Smf, Vf, Fd), and rivers (Sl). The morphometry results show that a young deformation in this area has caused on uplift in the crust along structures in the Alborz. The Garmsar area is more active than the Semnan area in which both are more active than the Eyvanekey area. All of the alluvial fan evolution in this area relate to the Quaternary events. The study on the information obtained from the exploitation wells and geoelectric profiles of the region shows that the Alborz uplift in the north is associated with the erosion and deposition of the new deposits in the form of alluvial fans. The bedrock behavior at the base of the fans has a direct effect on the formation of the second- and third-generation fans. The effect of the continual compressional tectonics in the Late Quaternary is associated with the uplifting evaporite masses, the uplifting hanging walls of the reverse faults, and the growth of the folded structures.

Keywords Alluvial fans · Late Quaternary · Morphometry · Compressional tectonics · Alborz Mountains · Northern Iran

Introduction

The intracontinental Alborz range in Northern Iran (Djamour et al. 2010) is an active deformation and seismic zone (Jackson et al. 2002). The Alborz Mountains, with ~ 600 km length, ~ 100 km width, and an almost eastern–western direction, is located on the southern margin of the Caspian Sea and the northern Central Iran. This range is extended from the Ararat Mountains in the west and joins the Hindu Kush Mountains in Afghanistan in the east, passing through the north of Iran (Allen et al. 2003). Alborz is divided into the three parts: Western, Central, and Eastern Alborz (Stöcklin 1974). The Central and Eastern Alborz are active orogenic belts. They are located on the northern part of the Arabia–Eurasia collision zone. The deformation in these areas indicates that from the Late Cenozoic, they have been affected by oblique shortening in the NE direction (Jackson and Mckenzie 1984; Allen et al. 2003). Based on the tectonic observation (Allen et al. 2003; Ritz et al. 2006) and seismicity (Jackson et al. 2002), oblique motion across the Eastern and Central Alborz is partitioned to left lateral strike slip faulting and thrust faults, which are parallel to the belt (Jackson et al. 2002; Allen et al. 2003). The epicenter of recent earthquakes and the documented historical seismicity (Ambraseys and Melville 1982; Berberian and Yeats 1999) in the Central and Eastern Alborz indicate that there is an active zone with various fault activities (Tchalenko 1974; Berberian 1976; De Martini et al. 1998; Berberian and Yeats 1999; Ashtari et al. 2005). More fault focal mechanisms are reverse, and some such as the Mosha fault is reverse with a sinistral component (Ashtari et al. 2005). The depth of most earthquakes is between 10 and 20 km and, therefore, is not deep and mostly limited to the crust (Jackson et al. 2002; Berberian and Yeats 1999).

Responsible Editor: François Roure

✉ Soheila Bouzari
s_tectonic@iau-tnb.ac.ir; s_tectonic@yahoo.com

[1] Department of Geology, Islamic Azad University Tehran North Branch, Shahid Babaei Highway- Hakimiyeh exit- Shahid Abbaspour Boulevard, Tehran 1651153311, Iran

Most studies in the Central and Eastern Alborz focus on structural analysis, deformation, and seismic activity in a large scale. The fan morphology, catchment basin area, mountain front, and morphology of rivers are very little known in the Central and Eastern Alborz. Poor morphology data in these areas are a strong motivation in this study. Based on the testing morphometric indexes, various features of the shortening crust and the compressional deformation occurred on the southern margins of the Central and Eastern Alborz in the Late Quaternary. In this study, we focused on the fan morphology as evidence for understanding the young activity in these areas. Fans are the key landforms that are sensitive to the functions of external and internal factors of the crust of the Earth. They are common landforms that usually form along highland areas such as mountain ranges, faulted and folded structures, and regions uplifted by salt domes (Heward 1978; Gloppen and Steel 1981; Blair 1987; Moreno and Romero-Segura 1989; Silva et al. 1992, 2003; Nemec and Postma 1993; Srivastava et al. 1994; Mack and Leeder 1999; Robustelli et al. 2002; Benvenuti 2003; Viseras and Fernandez 1994; Viseras et al. 2003; Singh and Tandon 2007; Sancho et al. 2008; El Hamdouni et al. 2008; Goswami et al. 2009; DeCelles 2011; Bahrami 2013). Such fans formed the southern front of the Central and Eastern Alborz Mountains (Fig. 1a). Alluvial fans have mostly eroded from high elevations in the north and have been deposited on the front of Alborz (Fig. 1b, c). The depositional process is a factor for classifying alluvial fans as area debris flow (Robustelli et al. 2002) and mountain front fans (Harvey 1988; Robustelli et al. 2002).

The morphology, morphometry, and the development of the alluvial fans are controlled by factors such as tectonic activity (Whipple and Tucker 1999; Calvache et al. 1997; Li et al. 1999; Viseras et al. 2003; Harvey 2005, 2012; Goswami et al. 2009; Bahrami 2013; Castillo et al. 2017), climate (Beaumont 1972; White et al. 1996), lithology (Lecce 1991; Blair and McPherson 1998; Berlin and Anderson 2007; Limber and Barnard 2018), and base level change (Koss et al. 1994; Harvey 2002; Storz-Peretz et al. 2011; Limber and Barnard 2018; Struth et al. 2019). These alluvial fans are the major features of the compressional tectonics (Salfity et al. 1984; Rodríguez-Fenández et al. 1999; Sancho et al. 2008; Castillo et al. 2017) and other deformations during the Late Quaternary.

Alluvial fan morphometry allows us to distinguish the role of the faults, folds, salt growth, and positive and negative isostasy in the form and growth of the fans. The morphometric indexes of the fans indicate the newest signs of the reaction of the crust to the compressional tectonic effect in the Eyvanekey, Garmsar, Semnan areas, given clear vision to the reconstruction of the geodynamic evolution of the Central and Eastern Alborz and Central Iran during the Late Quaternary. The major question is to describe how the results of the Late Quaternary compressional tectonics affect the Central and Eastern Alborz based on the morphometric indexes, including the fan model in Eyvanekey, Garmsar, Semnan areas.

After an overview of the morphometric indexes, an important conclusion of this paper shows that Garmsar area in the Central Alborz is more active than the Semnan and Eyvanekey areas. This means the Central Alborz is formed from two parts: the west and east Central Alborz in which the east Central Alborz is more active than the west Central Alborz. Moreover, the data of geoelectric profiles and exploitation wells indicate the role of bedrock to morphology of the fan and spreading in the front of the Central and Eastern Alborz Mountains.

Geological setting

The Alborz Mountains were affected by Katangai orogeny during the Late Precambrian (Stöcklin 1968; Nabavi 1976; Berberian 1976; Berberian and Yeats 1999). Metamorphism, folding, and deep faulting were formed during this orogeny. Along these faults, magmatic activity has occurred in the Western and Eastern Alborz. During this period, the Alborz part of the Gondwana passive margin (Guest et al. 2006a) and a shallow continental sea extended there. Based on the activity of the faults, horst and graben structural form formed on the Central (Assereto 1963) and Eastern (Stampfli 1978) Alborz Mountains. They structured a suitable area for exposing intrusive and extrusive magma. Based on the magmatic activity, the Alborz crust rifted away from the Gondwana during the Ordovician to the Silurian (Guest et al. 2006b) and continued further into the Lower Devonian. Therefore, the transgression of the sea developed during the Hercynian epirogenic activity. The Paleotethys oceanic crust subducted under the Turan continental crust (e.g., Stöcklin 1968; Stampfli 1978). The Paleotethys ended, and the Alborz collided with Eurasia during the Triass (Stöcklin 1974; Stampfli 1978; Berberian and King 1981). The suture zone is probably situated along the northern front area of the Alborz (Guest et al. 2006a). During the Early Cimmerian orogeny, the Alborz area and especially the Eastern Alborz rapidly uplifted (Stöcklin 1968). Simultaneously or possibly shortly after the closure of the Paleotethys in Northern Iran, the Neotethys entered the rift phase in Southern Iran. The Alborz zone was affected by the compressional tectonics as the Neotethys ocean closed and the Arabian plate had collided with the Eurasia plate during the late Eocene to early Oligocene (Berberian 1983; Haghipour et al. 1987; Berberian and Yeats 1999; Alavi 1996; Axen et al. 2001; Jackson et al. 2002; Allen et al. 2003; Agard et al. 2005; Guest et al. 2006a, b, 2007; Zanchi et al. 2006; Ritz et al. 2006; Vincent et al. 2007; Allen and Armstrong 2008; Horton et al. 2008; Rezaeian et al. 2012; McQuarrie et al.

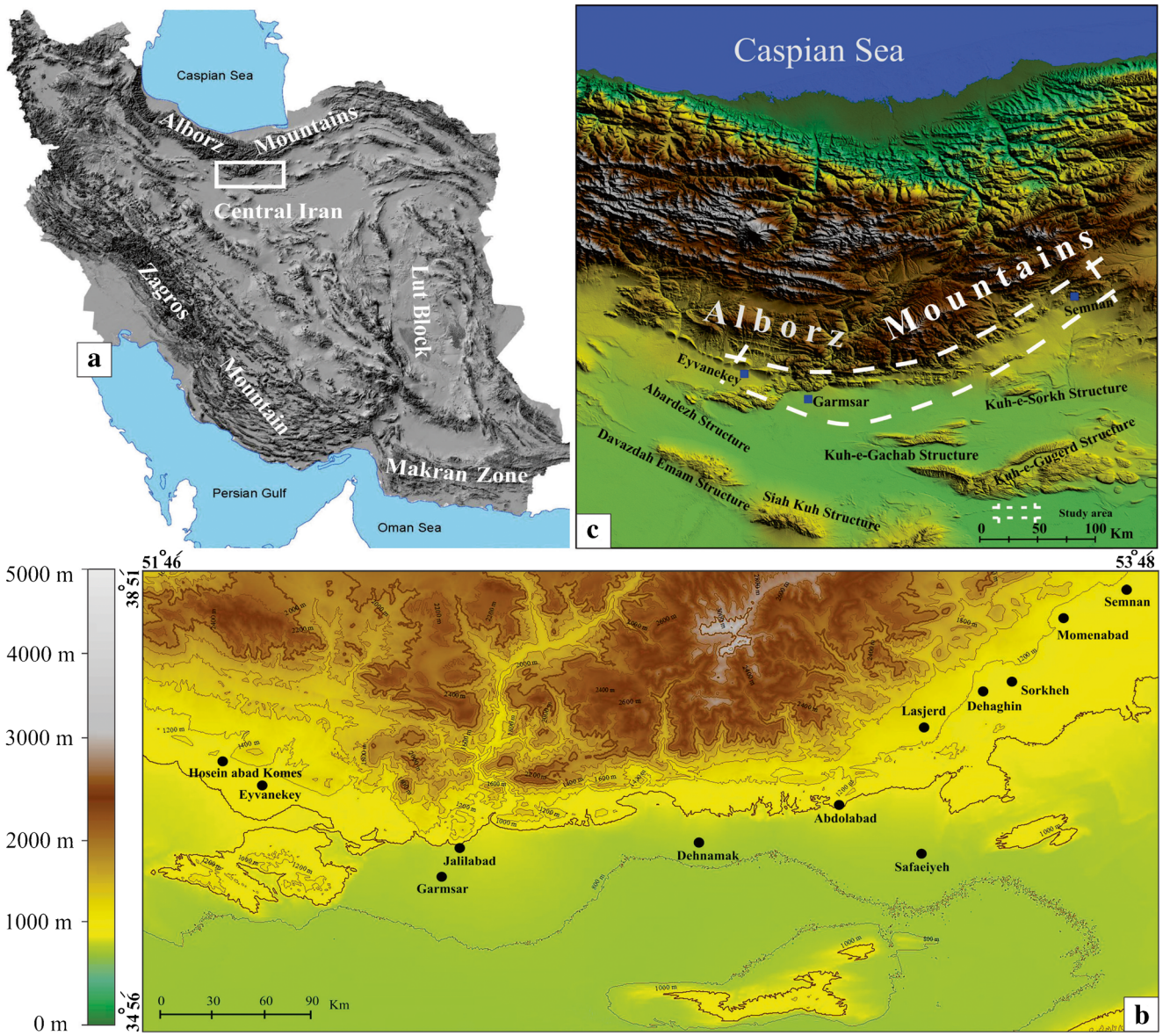

Fig. 1 **a** Geographical position of study area (white rectangle) over SRTM image. **b** Topographical map of the study area. Northern high and low areas reveal how fans occur at the boundaries of these areas. **c** Close up of the study area, Eyvanekey in the west, Semnan to the east, and Garmsar in the middle area, are denoted by a white dashed line

2003; Ballato et al. 2013, 2015; Francesca et al. 2014). The Alborz zone was strongly affected by the Laramid orogenic activity during the Paleocene, and the northern Alborz protrusion developed and shaped from the water. Furthermore, the Laramid orogeny in the Alborz is associated with thrust faults, folds, and rising intermountain sedimentary basins. During the sea transgression, conglomerate and sandstone have covered a major area of the Alborz. During early to middle Eocene, a shallow sea had developed at the southern area of the Alborz Mountains, and the Central Alborz composed of submarine basaltic eruptions with andesitic, dacitic, and tuffit rocks with a thickness of over 1500 m (Annells et al. 1975). The Pyrenean orogeny during the late Eocene and early Oligocene accompanied the compressional tectonics and the uplifting crust in the Alborz. Based on this orogeny, the Oligocene units did not form in the Central Alborz Mountains (Dellenbach 1964). Furthermore, the Eocene rocks in the southern Alborz Mountains were covered unconformably by Miocene continental sediments. During Late Miocene, strong erosion affected the formation of the Alborz; therefore, a thick conglomerate of the Hezardareh Formation was deposited in the front area of the Alborz Mountains (Rieben 1966). During the late Alpine orogeny in Late Pliocene or Early Pleistocene, thrust faults and fold structures have developed in the Alborz (Nabavi 1976, 1998; Pedrami 1987; Westaway 1994; Allen et al. 2004; Hosein-Khannazer 2015). This indicates the association of the shortening of the crust and the compressional tectonics with the

uplifting of the Alborz (Allen et al. 2004; Guest et al. 2006b; Ballato et al. 2008, 2011, 2013; Van Hunan and Allen 2011; Mouthereau et al. 2012). Modern Global Positioning System (GPS) data confirm that the deformation of the Central Alborz is ~ 5 mm/year over 100 km (Vernant et al. 2004b) and a NNE maximum horizontal stress orientation (Allen et al. 2004; Vernant et al. 2004a, b; Masson et al. 2007) from Late Miocene to the Holocene is active in the Central Alborz. It is partitioned into the 5 ± 2 mm/year of the shortening crust and the 4 ± 2 mm/year left lateral shearing (Vernant et al. 2004a, b; Masson et al. 2007). The shortening crust in the southern of the Alborz is 3 mm/year (Vernant et al. 2004b), and that in the Eastern Alborz and Kopet Dagh is 14 ± 2 mm/year (Guest et al. 2006a), whereas in the Eastern Alborz, 3.5 mm/year is seen (Tavakoli 2007). The shortening crust in the Alborz is a range between 30 km (Allen et al. 2004) and 53 ± 3 km (Guest et al. 2006b). This fact is related to the regional 2 cm/year convergence rate of the Arabia–Eurasia collision (McQuarrie et al. 2003; Allen et al. 2004). The modern deformation in the western area of the Central Alborz is due to the transpressional deformation which is consistent of the thrust and the left lateral faults (Vernant et al. 2004b; Guest et al. 2006a).

Methods

In order to study the youngest deformations of the Central and Eastern Alborz regions in response to the compressive tectonics, the morphology of the fans has been studied in the Eyvanekey, Garmsar, and Semnan areas. For this purpose, in addition to the surface evidence and studies, subsurface evidences have been investigated.

In the studies on the surface, a digital elevation model (DEM) was first developed. After a comparison and applying it to QuickBird satellite images (with a precision lower than 1 m), the polygons of the fans and the catchment basins were determined. The structure of the area, including folds and faults along with the evaporite masses, was extracted from Tehran and Semnan geological maps in a scale of 1:250,000 and from Semnan and Garmsar maps in a scale of 1:100,000 (prepared by the Geological Survey of Iran). The structural map was combined with the SRTM images (Shuttle Radar Topography Mission) to determine the structural position of the fans and their catchments. As a result, 17 morphometric indexes (Table 1) were measured for 131 fans (alluvial and debris), 26 catchment basins, rivers, and the mountain frontal area of the Central and Eastern Alborz Mountains.

Fan area (F_a) indicates the total planimetric area of each fan. Fan slope (F_g) is the gradient measured along the axis of each fan. The ratio of the width/length of the fan (WLF) was determined, which expresses the elongation of the fan (Viseras and Fernandez 1994). Fan cone (F_c) shows the conical shape (Mukerji 1976). Sweep angle (A_s) indicates the angle between the outermost positions of the channels of a fan (Viseras and Fernandez 1994). Fan radius (R) shows the maximum radius of each fan. Fan symmetry (F_s) indicates the fan symmetry (Keller and Pinter 1996). Catchment basin area (D_a) shows the total planimetric area of each fan. Catchment basin shape (B_s) indicates the elongation of the basin. The ratio of length/width of the basin was determined (El Hamdouni et al. 2008). Stream length gradient (Sl) indicates the slope variation along the length of the river (Keller and Pinter 1996). The topographic symmetry factor of each basin is shown with the variable T (Keller and Pinter 1996). Basin asymmetry (AF) shows the percentage of asymmetry of each basin (Keller and Pinter 1996). Index of cut (Fd) shows the percentage of the cutting mountain front of each mountain (Bull 2007). Multifaceted surface (Fmf) indicates the percentage of the multifaceted surface to the straight line of the mountain front (Bull 2007). The ratio of floor/height of the valley (Vf) indicates the valley of the fan (Azor et al. 2002). The ratio of sinuosity/straight line of the mountain front (Smf) expresses the sinuosity of the mountain front (Keller and Pinter 1996). Longitudinal profile (Bull 1964) shows the change of alluvial fan slope along the longitudinal profile.

In the substructure study, in order to recognize the characteristics of the fan bedrock (based on geoelectric data of the Semnan Province water organization), geoelectric sections of Eyvanekey, Garmsar, Dehnamak–Safaeyeh, and Sorkheh–Semnan were sketched. Moreover, to determine the sedimentary sequence of the fans, a stratigraphic column was drawn based on the data from the exploitation wells. During field work, evidence of young crustal movement in the fans was examined and occasionally measured.

Thus, by linking the results obtained from the surface studies, subsurface investigation, and field work, the model of the Eyvanekey, Garmsar, and Semnan fan development was provided.

Results

To understand the alluvial fan evolution, the study area has been split into three areas: Eyvanekey, Garmsar, and Semnan (Fig. 2). The Eyvanekey and Garmsar areas formed in the Central Alborz with an E–W trend, and the Semnan area formed along the Eastern Alborz with an NE trend. Most alluvial fans were formed by rivers that flow through the Alborz Mountains. Following the morphometric indexes, for the fans, catchment basins, mountain front, and rivers in three areas are interpreted.

Table 1 Parameters used in the morphometric analysis of fans, catchment basins, mountain fronts, valleys, and rivers

Symbol	Parameter	Unit	Meaning
F_a	Fan area	km^2	Total planimetric area of each fan
F_g	Fan slope (gradient)	Nondimensional	Gradient measured along the axis of each fan
WLF	Ratio of width/length of the fan	Nondimensional	Expresses the elongation of the fan
FC	Fan conically	Nondimensional	Expresses the conical shape
A_s	Sweep angle	Degree	Angle between the 2 outermost positions of the channels of a fan
R	Fan radius	m	Maximum radius of each fan
F_s	Fan symmetry	Nondimensional	Expresses the fan symmetry
D_a	Drainage basin area	km^2	Total planimetric area of each basin
B_s	Drainage basin shape	Nondimensional	Expresses the elongation of the basin
Sl	Stream length gradient	Nondimensional	Expresses the elongation of the river
T	Topographic symmetry reverse	Nondimensional	Topographic symmetry reverse of each basin
AF	Basin asymmetry	%	Percentage of symmetry measured of each basin
Fd	Index of cut	%	Percentage of cutting mountain front of each mountain
Fmf	Multifaceted surface	%	Percentage of multifaceted surface to straight line of mountain front
Vf	Ratio of floor/height of the valley	Nondimensional	Expresses the valley of the fan
Smf	Ratio of sinuosity/straight line of the mountain front	Nondimensional	Expresses the sinuosity of the mountain front
Bull	Longitudinal profile	Nondimensional	Expresses the fan group

Eyvanekey area

In the Eyvanekey area, two alluvial fans have been formed: the Komes fan with ~ 14 km^2 area and the Eyvanekey fan with > 85 km^2 area from the west to the east, respectively (Fig. 2). They are fed by the Komes and Eyvanekey rivers and originate in the Kalarz and Hoseinkhani mountains 2331 m into the Central Alborz Mountains.

The Eyvanekey area is bordered by the Eyvanekey–Parchin fault from the north, Varamin plain to the west, the Sardareh evaporite mass to the east, and the Abardezh fault and folded structure to the south (Fig. 2). In the northern part of the Eyvanekey–Parchin fault, the highland area with 1500 m height is formed. There is a catchment basin area of the Eyvanekey area. It is composed of Paleozoic rocks such as limestone, sandstone, and sandy shally marl. This is followed by Eocene tuff units, green and black shales, sandstone, conglomerates, and limestone. It is covered by Oligocene evaporite sedimentary units, and Miocene Upper Red Formation with sedimentary rocks. Hezardareh conglomerate and sandy

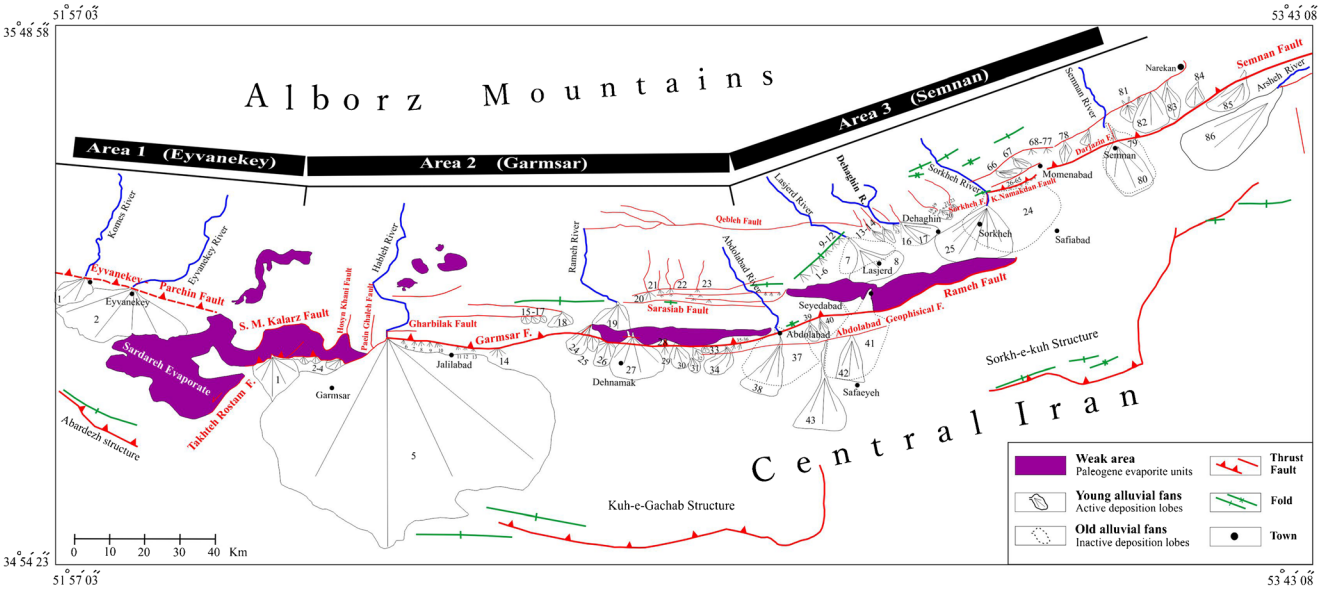

Fig. 2 Structural features of the study area (based on Haghipour et al. 1987; Aghanabati and Hamedi 1994) with three area fans of the Eyvanekey, Garmsar, and Semnan and fan number

conglomerate units of the Kahrizak Formation are shown in Fig. 3.

Toward the southern part of the Eyvanekey–Parchin fault, there is the Central Iran area which is covered by Quaternary deposits and the alluvial fans of the Eyvanekey area formed in the area. The bedrock of the alluvial fans based on geoelectric section (Fig. 4a) is made from gypsum units from the Lower Red Formation. Also, the Komes alluvial fan stratigraphy column that is prepared based on the exploitation well 28 (Fig. 5) is formed from fine and coarse sand with clay and gravel.

The morphometric indexes have been measured for the Eyvanekey area. Based on the study of Bull (1964), the Eyvanekey fan is in group B and the Komes fan in group C. The A_s values (Table 2) change from 95° to 137° for the Komes and Eyvanekey fans, respectively. The WLF is 0.671 in the Komes fan and 1.232 in the Eyvanekey fan. They are fed by the permanent rivers, and the fan slope (F_g) in the Eyvanekey area is < 2 (Table 2). The radius (R) is 977 to 992 m in the Komes and Eyvanekey fans, respectively. The fan cone (FC) index in the Eyvanekey fan and Komes fan is 1.101 and 0.751, respectively. The F_s value or fan symmetric index in the Komes fan is 65.693 relatively bigger than that in the Eyvanekey fan which is 49.241. The valley width-to-height ratio (Vf) for the Eyvanekey River is 2.451, and that for the Komes River is 2.358. The sinuosity of the Central Alborz Mountains in the Eyvanekey area is 1.263. Also, the Fmf and Fd indexes are 4.178 and 0.312, respectively. Catchment basins in the Eyvanekey area are located in the Central Alborz area, and their morphometric indexes with the stream length gradient (Sl) are shown in Table 2.

Garmsar area

The Garmsar area includes 43 fans, 12 of which are alluvial fans and the rest debris fans (Fig. 2). Due to the evaporite units and fault structure, the Garmsar fans were distributed in 7 subareas (Table 2) (Garmsar 1–5, Jalilabad 6–14, Sarasiab 15–19, northern Sarasiab 20–23, western Dehnamak 24–27, eastern Dehnamak 28–36, and Abdolabad 37–43) (Table 2). At least three fan generations have been identified in the Garmsar area (Fig. 2).

The Garmsar area is bounded by the Eyvanekey area to the west, the Semnan area to the east (Fig. 2), and the Central Alborz Mountains to the north. Firuzkuh with 1900 m and Gharbilak with 997 m are the highest and lowest mountains in this area, respectively.

The Garmsar thrust fault zone on the E–W trend is the main border between the Central Alborz area in comparison to an uplifted area in the north and the Central Iran toward the south. In this area, catchment basins are on the northern side. The Eocene rocks are the oldest outcrop in the uplifted catchment area. It consists of tuff, green and black shale, sandstone, conglomerate, and limestone. They are continued by Oligocene sandstone, conglomerate, marl and gypsy marl, and Miocene units. The Miocene units include the Upper Red Formation, consisting of red and velvet marl, gypsum, sandstone, shale, conglomerate, and light brown to reddish brown shale. The youngest units of this section are Miocene–Pliocene conglomerate and Pliocene–Pleistocene sandstone, conglomerate, and marl (Fig. 3).

The Central Iran in the Garmsar area is covered by Quaternary deposits. The bedrock of the Garmsar area based on the geoelectric sections (Fig. 4b, c) is composed of

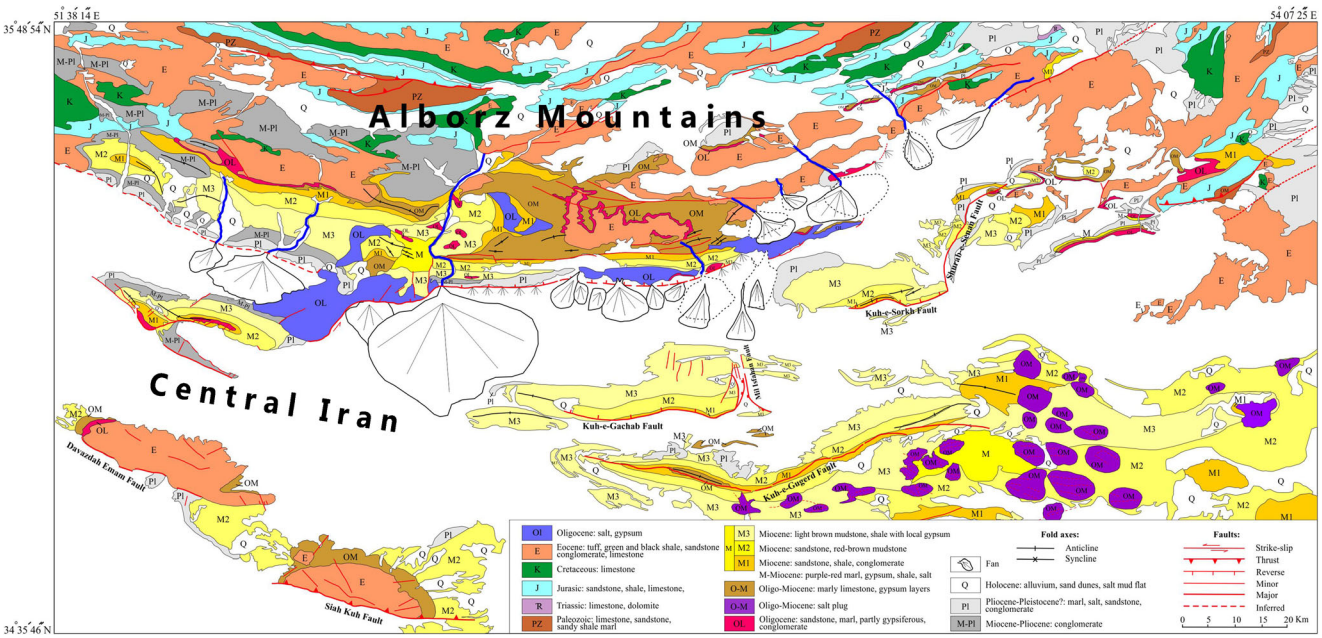

Fig. 3 Simplified geological map of the study area (after Bouzari et al. 2013)

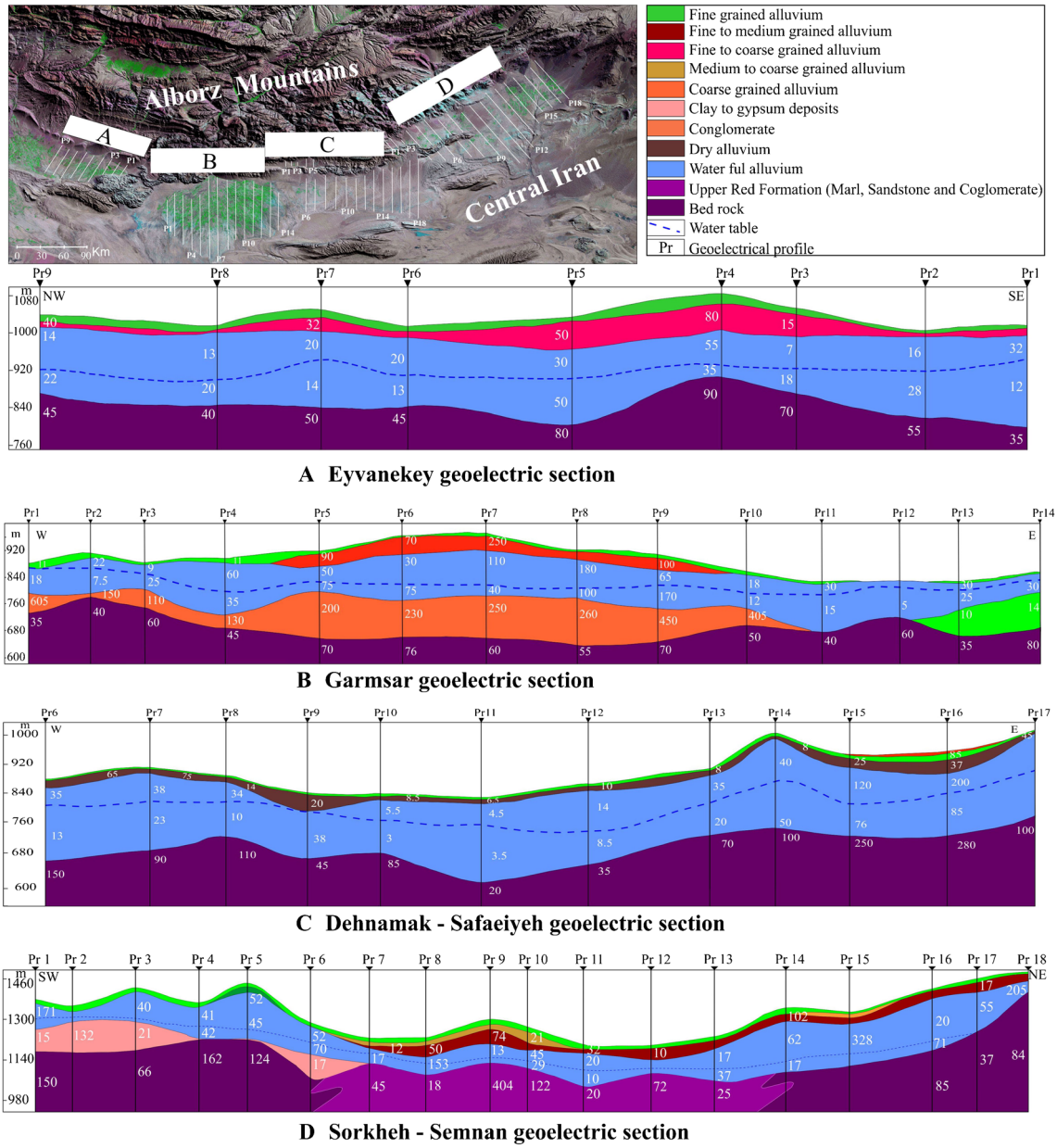

Fig. 4 Geoelectric sections in the study area. **a** The Eyvanekey area with bedrock uplift near Sardareh evaporite mass. **b** The Garmsar area with lenses, although relatively smooth. **c** The Dehnamak to Safaeyeh area showing relatively smooth bedrock and uplift near evaporite mass. **d** The Sorkheh to Semnan area showing bedrock made by block faulting

Oligocene gypsum units of the Lower Red Formation. The stratigraphic column of well (48) (Fig. 5) on the western Garmsar fan and well (36) of the Garmsar fan mostly consists of gravel, conglomerate, and sandy conglomerate. The alluvial fan deposits in the wells (37, 26), the Jalilabad (well 40), and the old channel of Dehnamak (well 53) are generally composed of sandy clay, sandy mud, clay, and coarse sand (Fig. 5).

In the Garmsar area, morphometric indexes are measured for 43 fans, catchment basins, rivers, and the mountain front. According to the index of Bull (1964), about 40% of fans of this area are of group B, about 50% of the others are of group C, and 10% are of group D. The WLF and A_s indexes for the Garmsar subarea fans show a variety of conditions. In the Garmsar, Jalilabad, Sarasiab, western and eastern Dehnamak, and Abdolabad fan subareas, A_s was > 60 and WLF < 1. The exception is Garmsar fan (5) at WLF > 1 and A_s > 50 which is in group A, according to the study of Viseras and Fernandez (1994) and Viseras et al. (2003). In some cases, such as the debris fans of the northern Sarasiab, A_s was ≤ 50 and WLF was < 1. The alluvial fan area (F_a) ranges from a maximum of 761.561 km^2 in the Garmsar fan to 3.685 km^2 in fan 23 in north Sarasiab (Table 2). The catchment basin area (D_a) in the Garmsar area is in a range between 1092.702 km^2

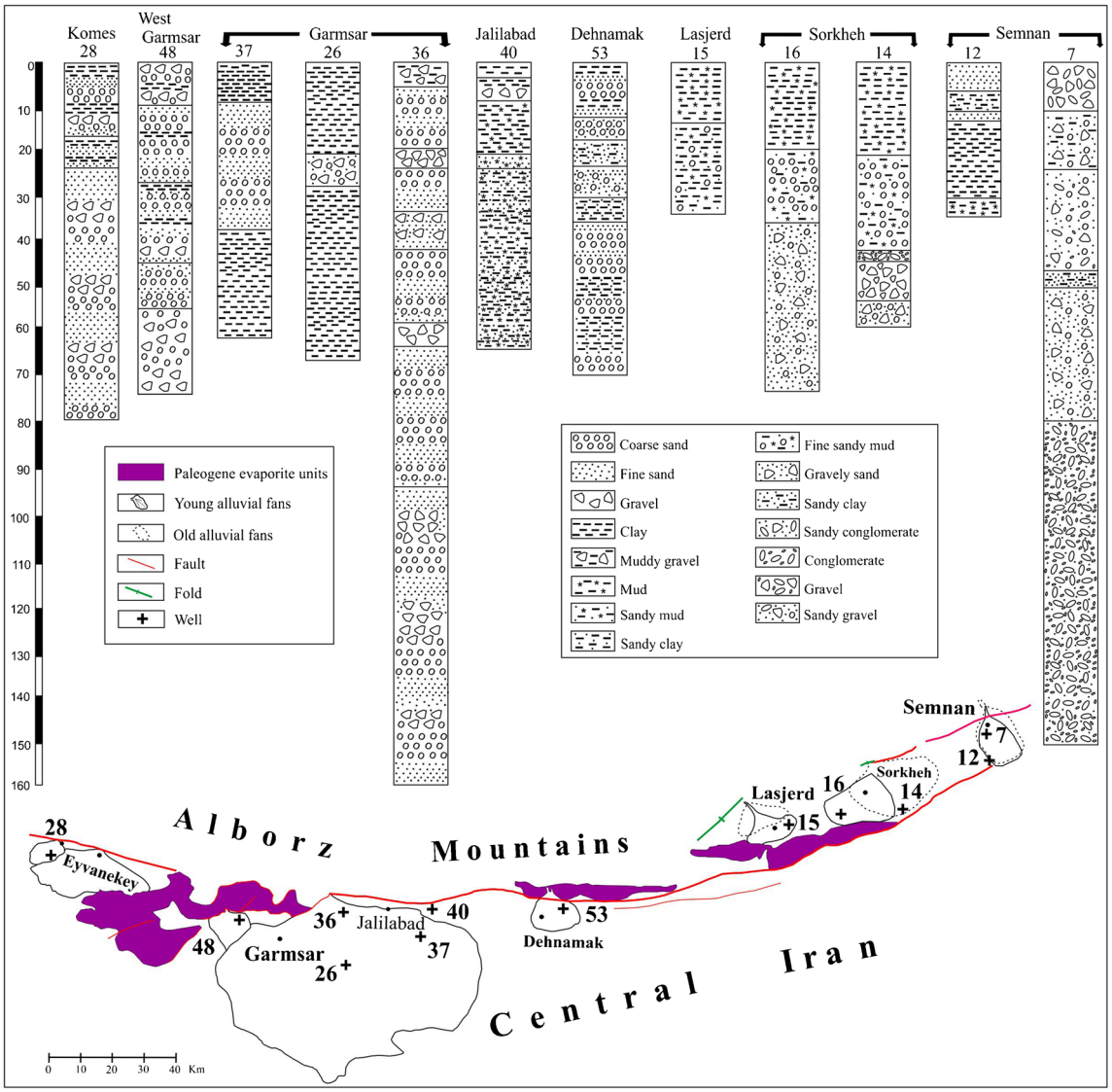

Fig. 5 Exploitation wells in the study area. Wells 7 and 36 show alluvial lithological characteristics maximally to 160 m in depth. Alluvial sequences are primarily coarse at elevation, showing uplift in this area. Well 26 shows alluvial channels in Garmsar fan. Well 15 in Lasjerd fan shows flooding current deposits in the area. The fine grading sequence in wells 14 and 16 in Sorkheh fan and in well 12 in Semnan fan shows the effect of factors such as fan inclination

in the Garmsar fan (5) and 20.042 km^2 for fan 30 (Fig. 6, Table 2). The fan slope (F_g) of alluvial fans varies from 1° to 5°, but generally, the index of < 2 for debris fans has increased. The FC index value in the Garmsar area is mostly < 1, but for fans 6, 9, 18, and 21–23, the value is > 1. Based on Table 2, the F_s index is mostly < 50, but in some fans, it is > 50, for example in fans 3, 6, 9, 15, and 39. The Vf index for the Garmsar area rivers (Table 2) ranges from 1.673 for the Hableh River and primarily a V-shaped valley in the west to 0.544 for Abdolabad River and a U-shaped valley in the east (Fig. 2). The Vf index in the Sarasiab subarea seasonal stream is 0.279. The Smf index ranges from 1.008 in the Jalilabad subarea in the west to 1.422 in the Dehnamak to Abdolabad subareas in the east. The multifaceted mountain front index (Fmf) is in a range between 2.857 in the Jalilabad and 8.894 in the western Garmsar area. The Fd index is < 1 for the other subareas, except the west Garmsar and Garmsar subareas with 1.231 and the Jalilabad with 1.124. The AF index is generally > 50, and the *T* index is between 0.361 in fan 43 and 0.791 in fan 19. Based on the catchment basin shape (BS) index, catchment basin for fans 27 and 42 have maximum (4.256) and minimum (1.355) elongation, respectively. The other morphometric indexes are shown in Table 2.

Semnan area

In the Semnan area, the 86 fans identified are classified into three generations and 8 subareas (Table 2): southern Lasjerd

Table 2 Data from morphometric analysis of fan, catchment basin, mountain front, and river populations

Fan	WLF	A_s (°)	FA (km^2)	BA (km^2)	F_g	R (m)	FCI	FS	Vf	Smf	Fmf	Fd	AF (%)	T	Sl	BS	Bull (1964)	Viseras et al. (2003)
Area 1																		
Eyvanekey																		
1	0.671	95	13.912	28.710	1.237	977	0.751	65.693	2.358	1.263	4.178	0.312	47.932	0.168	65.702	1.600	C	C
2	1.232	137	85.521	168.371	1.074	992	1.101	49.241	2.451				47.751	0.245	120.000	1.000	B	A
Area 2																		
2-1: west Garmsar and Garmsar																		
1	0.750	135	23.451	43.146	0.639	4646	0.631	27.415	1.092				59.811	0.473	323.433	1.621	A	C
2	0.891	90	0.838	–	3.775	1047	0.783	50.185	1.381				–	–	–	–	D	C
3	0.421	90	0.305	–	2.071	659	0.371	60.399	–	1.272	6.076	1.231	–	–	–	–	B	C
4	0.523	40	2.027	–	1.413	1828	0.423	42.936	0.581				–	–	–	–	B	B
5	1.112	100	761.561	1092.702	4.501	28,831	0.664	27.063	1.673		8.894	1.213	52.210	0.437	246.120	3.484	B	A
2-2: Jalilabad																		
6	0.281	50	0.390	–	38.071	551	2.639	62.796	–				–	–	–	–	D	B
7	0.533	55	1.159	–	32.157	1114	0.753	50.944	0.487				–	–	–	–	A	B
8	0.199	33	0.292	–	34.727	1286	0.923	66.894	0.689				–	–	–	–	A	B
9	0.631	50	1.028	–	31.754	1623	1.175	54.573	4.609				–	–	–	–	A	B
10	0.912	85	1.600	–	33.289	1385	0.849	37.465	2.259	1.008	2.857	1.124	–	–	–	–		C
11	0.544	70	0.713	–	32.915	1004	0.758	–	1.067				–	–	–	–	C	C
12	0.731	90	0.512	–	43.025	582	0.651	–	0.588				–	–	–	–	D	C
13	0.780	85	0.246	–	49.671	497	0.743	–	–				–	–	–	–	A	C
14	0.872	100	4.351	21.553	23.406	1588	0.666	–	–				–	–	–	–	B	C
2-3: Sarasiab																		
15	0.423	60	0.645	–	4.087	1232	0.987	56.727	–				–	–	–	–	D	C
16	0.752	82	0.893	–	3.735	1178	0.899	20.179	–				–	–	–	–	C	C
17	0.721	80	0.722	–	4.231	996.8	0.833	28.110	–	1.058	3.653	0.836	–	–	–	–	C	C
18	0.891	90	4.373	17.976	1.890	2470	1.129	41.092	–				70.762	0.527	95.685	2.130	B	C
19	0.840	100	12.069	124.712	2.973	4300	0.987	Circular	0.279				63.124	0.791	618.974	2.047	C	C
2-4: north Sarasiab fault																		
20	0.873	126	2.226	–	0.490	1624	0.983	–	0.511	1.241	5.219	0.837	–	–	–	–	A	C
21	0.452	50	1.088	–	5.221	1668	1.042	39.465	0.564				–	–	–	–	D	B
22	0.401	80	0.711	–	4.501	1583	1.021	17.557	1.865				–	–	–	–	C	C
23	0.782	90	3.685	–	5.142	1844	1.539	–	0.986				–	–	–	–	C	C
2-5: west Dehnamak and Dehnamak																		
24	0.458	40	7.761	–	1.832	3758	0.753	–	–	1.442	5.594	0.819	–	–	–	–	C	B
25	0.358	90	2.950	–	2.161	1963	0.734	–	–				–	–	–	–	C	C

Table 2 (continued)

Fan	WLF	A_s (°)	FA (km^2)	BA (km^2)	F_g	R (m)	FCI	FS	Vf	Smf	Fmf	Fd	AF (%)	T	Sl	BS	Bull (1964)	Viseras et al. (2003)
26	0.551	143	7.386	–	2.010	3321	0.867	–	0.531				–	–	–	–	B	C
27	0.790	90	32.206	35.852	1.661	6489	0.970	36.989	1.136				53.712	0.487	590.799	4.256	B	C
2-6: east Dehnamak																		
28	0.621	65	1.181	–	2.610	1718	0.776	–	1.265				–	–	–	–	C	C
29	0.615	90	0.854	–	1.411	1537	0.526	–	4.027				–	–	–	–	D	C
30	0.580	65	6.699	20.042	1.201	4024	0.764	–	1.123				69.426	0.747	452.775	2.044	B	C
31	0.528	83	2.421	–	0.721	2845	0.586	–	–				–	–	–	–	C	C
32	0.519	41	1.988	6.388	1.141	2339	0.599	–	2.000	1.442	5.594	0.819	56.215	0.664	18.245	2.834	B	B
33	0.428	62	0.089	–	2.340	895	0.771	–	–				–	–	–	–	B	C
34	0.552	75	9.847	13.274	0.831	4922	0.691	–	0.869				77.558	0.509	178.965	1.625	C	C
35	0.736	69	0.511	–	1.793	1134	0.764	–	–				–	–	–	–	C	C
36	0.422	65	0.318	–	0.043	1178	0.589	–	–				–	–	–	–	D	C
2-7: Abdolabad–Seyedabad																		
37	0.788	109	55.181	140.570	1.781	7432	1.239	22.055	3.273				58.712	0.480	1106.177	3.597	B	C
38	0.379	35	22.753		1.363	8503	0.893	22.055		1.442	5.594	0.819					B	B
39	0.525	90	3.525	–	2.790	2285	0.631	65.498	0.888				–	–	–	–	C	C
40	0.429	41	1.473	–	3.082	1841	0.760	72.443	1.556				–	–	–	–	C	B
41	0.480	45	65.032		10.441	12,226	0.573	32.772									B	B
42	0.398	49	16.012	220.461	1.145	6523	0.554	32.772	4.646				40.934	0.457	397.087	1.355	C	B
43	0.709	55	33.879	84.862	0.382	8175	0.756	–	–				62.136	0.361	136.709	3.241	B	C
Area 3																		
3-1: south Lasjerd anticline																		
1	0.535	79	1.901	–	2.761	1915	0.827	–	–	1.211	8.855	0.989	–	–	–	–	C	C
2	0.511	53	3.789	–	2.083	2038	0.592	–	–				–	–	–	–	C	C
3	0.467	41	0.958	–	3.824	1354	0.697	–	8.622				–	–	–	–	C	B
4	0.546	40	1.172	–	3.142	1542	0.777	–	10.445				–	–	–	–	C	B
5	0.431	60	0.493	–	6.053	726	0.056	–	10.131				–	–	–	–	B	C
6	0.694	105	0.145	–	6.762	372	0.611	–	2.601				–	–	–	–	B	C
7	1.178	105	23.736	220.152	2.691	4199	0.742	32.772	–				40.934	0.457	304.869	1.355	A	C
8	1.367	77	24.351		2.223	4272	0.765	32.772	2.815								B	C
3-2: east Lasjerd–west Dehaghin																		
9	0.518	92	0.996	–	3.281	1063	0.476	–	–				–	–	–	–	B	C
10	0.824	60	0.121	–	8.082	288	0.285	–	0.659				–	–	–	–	B	C
11	0.551	85	0.074	–	8.601	242	0.281	–	–				–	–	–	–	B	C
12	0.342	59	0.079	–	7.142	405	0.528	–	–	1.211	8.855	0.989	–	–	–	–	B	C

Table 2 (continued)

Fan	WLF	A_s (°)	FA (km^2)	BA (km^2)	F_g	R (m)	FCI	FS	Vf	Smf	Fmf	Fd	AF (%)	T	Sl	BS	Bull (1964)	Viseras et al. (2003)
13	0.427	74	1.202	–	3.162	1206	0.311	–	–				–	–	–	–	D	C
14	0.424	96	1.753	–	2.533	1160	0.234	–	0.764				–	–	–	–	D	C
3-3: Dehaghin																		
15	0.779	95	5.155	–	1.754	2968	0.712	–	–								A	C
16	0.513	90	16.903	–	1.811	5686	0.984	55.000	–	1.211	8.855	0.989	81.785	0.661	413.391	2.749	A	C
17	0.418	35	12.349	93.985	1.845	6086	0.854	56.105	2.779								A	B
3-4: east Dehaghin																		
18	0.489	25	0.116	–	3.995	760	0.586	–	–	1.211	8.855	0.989	–	–	–	–	C	B
19	0.492	69	0.203	–	2.253	996	0.699	–	–				–	–	–	–	C	C
20	0.901	90	2.011	6.202	2.340	1903	0.553	49.082	3.679				78.512	0.734	141.224	3.108	D	C
21	0.606	81	0.042	–	3.651	411	0.378	–	–				–	–	–	–	B	C
22	0.682	79	0.007	–	6.229	207	0.684	–	–				–	–	–	–	C	C
23	0.529	35	0.027	–	1.830	325	0.923	–	–				–	–	–	–	C	B
3-5: Sorkheh																		
24	1.238	135	87.829		1.592	10,000	0.941		1.379								B	A
25	1.051	70	50.548	266.06	1.374	9000	0.952		1.378	1.211	8.855	0.989	24.774	0.456	190.627	1.684	C	A
3-6: east Sorkheh (south Namakdan fault)																		
26	0.734	95	0.064	–	4.751	213	0.751	–	–				–	–	–	–	C	C
27	0.896	85	0.009	–	9.982	96	0.449	–	–				–	–	–	–	C	C
28	0.763	98	0.018	–	8.101	129	0.604	–	–				–	–	–	–	C	C
29	0.483	51	0.015	–	7.981	143	0.259	–	–				–	–	–	–	B	
30	0.521	50	0.035	–	7.293	214	0.664	–	–				–	–	–	–	C	B
31	0.613	70	0.012	–	8.733	98	0.579	–	–				–	–	–	–	B	C
32	0.522	86	0.039	–	6.011	125	0.267	–	–				–	–	–	–	C	C
33	0.578	56	0.086	–	5.462	412	0.751	–	–				–	–	–	–	B	C
34	0.625	57	0.009	–	9.911	126	0.543	–	–				–	–	–	–	D	C
35	0.427	55	0.005	–	9.291	78	0.269	–	–	1.063	3.063	1.038	–	–	–	–	C	C
36	0.279	51	0.139	–	8.770	113	0.569	–	–				–	–	–	–	C	B
37	0.315	54	0.132	–	8.363	175	0.507	–	–				–	–	–	–	C	C
38	0.312	51	0.139	–	8.792	189	0.736	–	–				–	–	–	–	C	B
39	0.831	56	0.065	–	2.594	201	0.447	–	–				–	–	–	–	B	C
40	0.347	69	0.025	–	3.972	359	0.718	–	–				–	–	–	–	B	C
41	0.662	52	0.069	–	4.121	367	0.665	–	–				–	–	–	–	C	B
42	0.484	95	0.054	–	6.072	228	0.353	–	–				–	–	–	–	C	C
43	0.492	88	0.036	–	5.792	192	0.177	–	–				–	–	–	–	C	C

Table 2 (continued)

Fan	WLF	A_s (°)	FA (km^2)	BA (km^2)	F_g	R (m)	FCI	FS	Vf	Smf	Fmf	Fd	AF (%)	T	Sl	BS	Bull (1964)	Viseras et al. (2003)
44	0.545	50	0.002	–	10.911	44	0.382	–	–				–	–	–	–	C	B
45	0.847	75	0.164	–	4.443	356	0.449	–	–				–	–	–	–	C	C
46	0.774	70	0.004	–	9.041	63	0.538	–	–				–	–	–	–	C	C
47	0.553	67	0.006	–	8.493	74	0.295	–	–				–	–	–	–	C	C
48	0.524	102	0.029	–	6.471	159	0.198	–	–				–	–	–	–	C	C
49	0.571	82	0.014	–	8.354	68	0.183	–	–				–	–	–	–	C	C
50	0.321	62	0.034	–	5.942	293	0.562	–	–				–	–	–	–	B	C
51	0.542	40	0.001	–	11.080	22	0.224	–	–				–	–	–	–	C	B
52	0.349	100	0.041	–	5.031	338	0.119	–	–				–	–	–	–	D	C
53	0.475	70	0.004	–	8.421	49	0.159	–	–				–	–	–	–	C	C
54	0.410	120	0.042	–	2.652	306	0.338	–	–				–	–	–	–	C	C
55	0.577	87	0.012	–	0.771	132	0.279	–	–				–	–	–	–	C	C
56	0.603	80	0.002	–	10.321	46	0.363	–	–				–	–	–	–	A	C
57	0.523	47	0.004	–	8.542	63	0.641	–	–				–	–	–	–	C	B
58	0.554	70	0.023	–	6.320	127	0.437	–	–				–	–	–	–	C	C
59	0.583	65	0.001	–	7.991	22	0.337	–	–				–	–	–	–	A	C
60	0.615	70	0.016	–	6.093	162	0.755	–	–				–	–	–	–	C	C
61	0.785	84	0.028	–	5.911	130	0.666	–	–				–	–	–	–	C	C
62	0.639	89	0.009	–	5.323	93	0.265	–	–				–	–	–	–	A	C
63	0.382	91	0.029	–	4.751	255	0.527	–	–				–	–	–	–	B	C
64	0.313	30	0.003	–	6.183	98	0.133	–	–				–	–	–	–	C	B
65	1.030	115	0.013	–	5.441	122	0.724	–	–				–	–	–	–	C	A
3-7: north Momenabad fault																		
66	0.410	110	2.848	5.632	1.761	2420	0.405	–	1.280				54.476	0.438	267.243	4.203	C	C
67	0.570	80	2.449	11.283	1.863	1417	0.151	–	1.439				57.733	0.391	570.740	2.492	B	C
68	0.601	85	0.102	–	1.920	329	0.455	–	–				–	–	–	–	A	C
69	0.413	60	0.076	–	4.933	334	0.342	–	–				–	–	–	–	D	C
70	0.453	75	0.099	–	4.241	345	0.339	–	–				–	–	–	–	C	C
71	0.415	105	0.247	–	3.362	600	0.528	–	–				–	–	–	–	D	C
72	0.285	66	0.145	–	3.401	668	0.542	–	–	1.152	5.880	0.934	–	–	–	–	C	C
73	0.449	87	0.124	–	4.056	406	0.295	–	–				–	–	–	–	D	C
74	0.256	45	0.327	–	2.411	802	0.154	–	–				–	–	–	–	D	B
75	0.653	80	0.152	–	2.772	442	0.826	–	–				–	–	–	–	C	C
76	0.440	40	0.140	–	2.282	488	0.377	–	–				–	–	–	–	A	B
77	0.443	45	1.201	–	2.383	1352	0.319	–	–				–	–	–	–	C	B

Table 2 (continued)

Fan	WLF	A_s (°)	FA (km^2)	BA (km^2)	F_g	R (m)	FCI	FS	Vf	Smf	Fmf	Fd	AF (%)	T	SI	BS	Bull (1964)	Viseras et al. (2003)
78	0.401	39	2.962	–	1.673	1594	0.234	65.879	7.022				54.099	0.195	229.042	1.689	C	B
3-8: Semnan																		
79	0.760	45	33.025	308.852	1.611	7950	0.620	49.545	1.706	1.152	5.880	0.934	47.612	0.279	324.130	1.199		
80	0.680	60	34.166		1.641	8284	0.901	40.513										
81	0.706	65	4.714	–	4.714	3002	0.403	36.631	–				–	–	–	–		
82	0.583	60	20.249	35.534	2.351	6701	0.699	35.183	2.649				61.139	0.545	578.104	4.775		
83	0.371	47	8.346	11.120	2.872	6507	0.341	53.609	–				36.097	0.692	98.584	1.723		
84	0.578	40	5.824	9.097	3.281	4073	0.522	–	–				51.314	0.370	187.672	1.970		
85	0.503	50	15.275	8.838	3.292	6849	0.288	28.385	0.685				60.274	0.228	69.253	1.569		
86	0.378	30	73.455	107.512	5.333	15,703	0.857	64.451	5.849				39.034	0.552	514.124	0.772		

anticline (1–8), eastern Lasjerd and western Dehaghin (9–14), Dehaghin (15–17), eastern Dehaghin (18–23), Sorkheh (24–25), eastern Sorkheh or southern Namakdan fault (26–65), northern Momenabad fault (66–78), and Semnan (79–86) (Fig. 2). Nine of these fans are alluvial fans, and the remaining ones are debris fans. The Semnan area is bordered to the west by Garmsar, to the east by the median uplift of the Semnan and Damghan basins, and to the north by the Eastern Alborz Mountains (Fig. 2). Kuh-e-Tang (> 2780 m) and Kuh-e-Royan (1890 m) are the highest and lowest northern mountains, respectively. The Lasjerd, Dehaghin, Sorkheh, and Semnan rivers flow straight from the Eastern Alborz Mountains to the southeast and southwest and feed alluvial fans (Fig. 2).

Semnan and Rameh fault zones serve as a border between the Eastern Alborz in the north and the Central Iran in the south. The Eastern Alborz has formed the uplifted catchment area. Jurassic sandstone, shale, and limestone are the oldest outcrops in this area. It is covered by Cretaceous limestone and Eocene units. The Eocene units are formed of milky green, black tuff; dacite; shale; and marl with an interbed of green–light gray coarse-grained sandstone, shear conglomerate, and very coarse sandstone (Fig. 3).

The Central Iran in front the fault zone is covered by Quaternary deposits. The characteristic of the bedrock of the Semnan area based on a geoelectric section (Fig. 4d) shows that the bedrock is formed from two parts: Eocene rhyolitic rocks with a specific resistance of 210–217 Ωm and Upper Red Formation with marl and sandstone with a specific resistance of 122–178 Ωm.

Based on the exploitation wells and stratigraphy column (Fig. 5), the deep well (~ 150 m) is in the Semnan fan (well 7) and the alluvial fan deposits are gravel, conglomerate, clay, and sandy clay to sand. Also wells 12 and 7 are in the distal and proximal parts of the Semnan fan, respectively. Well 15 in the new Lasjerd fan is mostly sandy clay. In the old and new Sorkheh fans (wells 14 and 16), the young deposits consist of gravel and conglomerate to sandy clay.

The investigation of morphometric indexes in the Semnan area (Table 2) indicates that based on Bull (1964), about 57% of fans are in group C, ~ 20% in group B, and 10% in group D and the remaining 13% have the ordinary condition or group A. The WLF index (Viseras and Fernandez 1994; Viseras et al. 2003) for 8 subareas (Table 2) was maximum 1.367 in fan 8 of the south Lasjerd anticline subarea. The index is < 1 in the other subareas, except the Sorkheh subarea (WLF > 1). The A_s value varies from 135° (fan 24) in the Sorkheh subarea to 25° (fan 18) in the east of the Dehaghin subarea. The maximum fan area (F_a index) is related to the Sorkheh subarea fans (24 and 25) with 87.829 km^2 and 50.548 km^2 areas. The catchment basin area (D_a) is maximum 308.852 km^2 in the Semnan subarea (Table 2). The slope of the fans (F_g) is generally between 2° and 5°. In some fans, for example fans in the

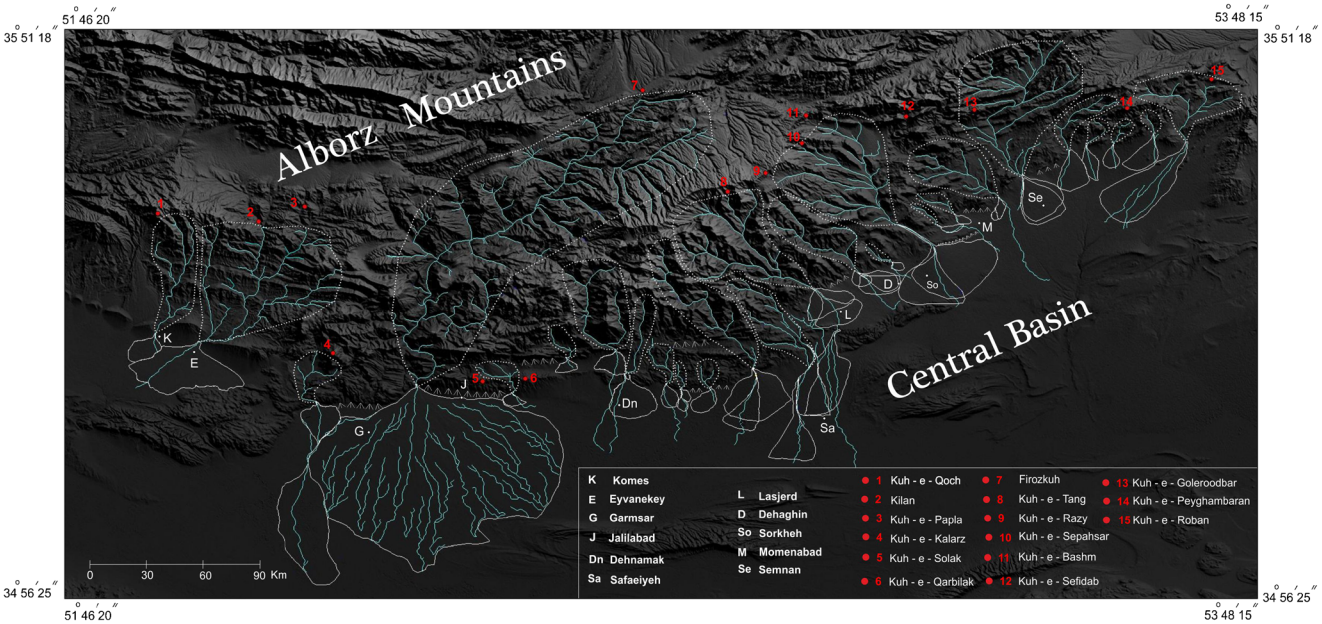

Fig. 6 Alluvial fans and catchment basins in the study area over SRTM image

south Namakdan fault subareas and Sorkheh fans, the index was > 5 and < 2, respectively. The FC index ranges from 0.119 (fan 52) to 0.952 (new Sorkheh fan 25). The F_s index is < 50 for the south Lasjerd anticline, east of Dehaghin subareas; > 50 for the Dehaghin and north Momenabad subgroups; and > 50 and < 50 for the Semnan subarea. The Vf index in this area is generally > 2. It is 1.379 in the Sorkheh and < 1 in the south Lasjerd anticline subareas. The Smf index in the south Lasjerd anticline to the east of Dehaghin subareas is 1.211. It changes to 1.152 in the Semnan and 1.063 in the east of Sorkheh subareas. The multifaceted surface index (Fmf) of the Eastern Alborz varies from 8.855 in the west to 3.063 in the south Namakdan fault subarea in the east. The Fd index varied from 0.989 to 0.934 in the west to the east of the Semnan area. It is 1.038 for the east of Sorkheh subarea. The AF index is both > 50 and < 50; for example, in the Sorkheh subarea, the index is < 50, but in the Dehaghin subarea, the index is > 50 (Fig. 6). The BS index is in a range between 1.199 and 4.775. It is 1689 in the Sorkheh subarea.

Interpretation

The characteristics of the alluvial fan of the bedrock at the depths of greater than 250 m (based on geoelectric profiles) show the alluvial part is composed of sand, clay, gravel, and conglomerate materials, and the bedrock is composed of Eocene rhyolitic rock and Upper Red Formation in Semnan and Oligocene gypsum units from the Lower Red Formation in the Eyvanekey and Garmsar areas. The Garmsar bedrock topography is similar to the Eyvanekey area. The bedrock depth is shallow in the north, near the Eyvanekey–Parchin and Garmsar fault zone, and its depth increased toward the southwest in the Eyvanekey area and east in the Garmsar area. In these areas, there are no sharp or sudden changes in lithology. In the Semnan area, the bedrock topography affects the fans' shape on the surface. In addition, the bedrock lithology suddenly changes from volcanic rocks as a high land to the Upper Red Formation as a subsided area (Fig. 4d). The information obtained from the 12 exploitation wells shows the sedimentary sequence in the Komes and Garmsar fans is similar to that in the Semnan fan. These sequences consist of fine sand, coarse sand, and gravel in the Eyvanekey and Garmsar fans. The sequence in the Semnan fan is mostly conglomerate, gravely sand, and gravel. In these fans, the grain size becomes primarily coarse as observed upward. As can be seen in Fig. 5, the stratigraphy column in wells 14 and 16 in the Sorkheh subarea is different with each other. It started with gravely sand, gravel, or conglomerate and continued with clay and sandy clay. The fine grain of the sedimentary sequence in the stratigraphy columns shows that erosion rate increased after uplifting (retrogradation). In addition, the sediment size is larger in the Eyvanekey–Parchin, Garmsar, and Semnan fault zones, and it changes to fine grain in the plains, located in front of the fault zone.

Based on the fan morphometric data analysis, uplifting in the Alborz Mountains coincides with sedimentation (B; Bull 1964) which is a common factor for forming fans in Eyvanekey, Garmsar, and Semnan areas (Table 3). Young mountain uplifting (C; Bull 1964) is more effective in the Komes fan in the Eyvanekey area and in the second-generation fans in the Garmsar and Semnan areas. Precipitation (D; Bull 1964) is another factor that is active in the Garmsar and Semnan areas. Based on Table 3 and according to Viseras and Fernandez (1994) and Viseras

et al. (2003), alluvial fans in the Eyvanekey area and first-generation fans in the Garmsar and Semnan areas (Fig. 2) with $A_s > 50$ were open and WLF > 1 formed in high tectonic subsidence. The second- and third-generation fans in the Garmsar and Semnan areas are mostly elongated, and they formed in low tectonic subsidence (WLF < 1, $A_s \leq 50$) and base level changes (WLF < 1, $A_s > 60$). In other areas except the Eyvanekey area with just one generation, second- and third-generation fans are formed over the previous fans. The second-generation alluvial fans in the Garmsar area (Garmsar, Abdolabad, and Seyedabad fans) are extended toward the Garmsar basin (Stöcklin 1968), and in the Semnan area, the fans extended toward the Semnan basin (Figs. 2 and 3). In the Sorkheh, Lasjerd, and Dehaghin subareas, fans extended to the local basin in the Semnan area. It is noticeable that the second-generation fans of Abdolabad (38), Seyedabad (42) in the Garmsar area, Lasjerd (8), and Sorkheh (25) in the Semnan area with a long neck were formed on the first generation. The Safaeyeh fan (43) is formed with long neck, too. Also, third-generation fans are formed along the minor faults such as the Sarasiab fault in the Garmsar area, the Kuh-e-Namakdan fault, and the Lasjerd anticline in the Semnan area (Fig. 2). Except the third-generation fans which are mostly debris fan without catchment basin, the first- and second-generation fans are alluvial fans and catchment basin for the second-generation fans is the same with that for the first-generation fans (Fig. 6). There is a direct relation between the first-generation alluvial fans and the catchment basin area (Fig. 7). According to Blissenbach (1954), the first- and second-generation fans are flat to gentle. They are fed by permanent rivers and are extended to wide area. The fan slope changed to steep for debris fans along the fault and fold structures. It is clear for debris fans in the Jalilabad and Sarasiab subareas in the Garmsar area and the south Lasjerd anticline, south of the Namakdan fault subareas in the Semnan area. The slope of the alluvial fans decreases toward the fault zone and increases and ends in a plain with a relatively slight slope. The agricultural land around the Eyvanekey, Lasjerd, Sorkheh, and Semnan is centralized in these areas. The fan cones are generally elongated (mean FC < 1) and asymmetric (mean $F_s < 50$) in the Garmsar and Semnan areas (Table 3) but are relatively complete and symmetric (mean $F_s \sim 50$, Table 3) in the Eyvanekey area. For instance, the west side of the Garmsar fan rose and extended toward the east, but the Abdolabad and Seyedabad fans extended to the west. In addition, the mountain front morphology analysis gives more detailed information for understanding active deformation in these areas. Based on the Vf index (El Hamdouni et al. 2008), the mean Vf index (Table 3) in the Eyvanekey area is U shape with low uplifting rate. In the west of Garmsar area, valleys are V shape (e.g., Hableh River) and U shape in the east (Abdolabad River). In the Semnan area except the Sorkheh River valley with V shape, the other valleys are U shape. Based on the study of El Hamdouni et al. (2008), the Semnan area is totally semi-active and the Garmsar area is active. The Sorkheh River's valley is narrower than the others. Although the Eyvanekey and Garmsar areas are a part of the Central Alborz, the Smf index is different in this area (Table 3). The Smf index in the Jalilabad and Sarasiab subareas is 1.008 in the northern part of the Garmsar thrust fault, and the rate of uplifting is larger than that of erosion. This rate is decreased toward the Dehnamak to Abdolabad subareas in the Garmsar area (1.442) and Eyvanekey area (1.263). Similarly, in the Semnan area, the rate of uplifting increased along the Kuh-e-Namakdan fault (1.063) and Lasjerd anticline and this is decreased to the eastern part of the Semnan subarea (1.152). There is a direct relation between the Fmf index value and evaporite mass. For instance, the Fmf index in the Jalilabad and east Sorkheh subareas is low with lack of evaporite units and it is increased in the west Garmsar subarea and Eyvanekey fan which are near the Sardareh evaporite mass. The maximum multifaceted index (Fmf) is related to the western part of the Semnan area (Table 3). The Fd index is minimum in the Eyvanekey area and maximum in the Garmsar area. Based on AF and *T* indexes, catchment basin in the Komes fan is symmetric, but in the Eyvanekey basin, it is relatively asymmetric; the left side of basin is uplifted (Fig. 6). In the Garmsar area, catchment basins are asymmetric and the right side are uplifted. In the Semnan area, it is similar and asymmetric (Fig. 6). The rivers in Eyvanekey, Garmsar, and Semnan areas feed from the north (Central and Eastern Alborz) and stream to the south, southwest, and southeast. Based on Sl index, Eyvanekey, Lasjerd, Semnan, and Dehaghin rivers and Abdolabad have maximum slopes. According to the B_s index, sudden uplift did not happen in the Eyvanekey area, but for first generation in Garmsar and Semnan areas, it has happened. As a result, the Eyvanekey catchment basin is not elongated.

Discussion

The Alborz Mountains located in the northern part of the Arabia–Eurasia collision is caused by the effect of compressional tectonics, since Late Miocene (Guest et al. 2006a). The results of the collision are uplifting, shortening, and thickening of the continental crust in this region (Allen et al. 2004; Guest et al. 2006b). The structural model of the Central Alborz presented by Stöcklin (1968), Alavi (1996), Allen et al. (2003), and Guest et al. (2006a). In the mentioned model, the main structures along the north and south flanks of the Alborz are presented.

Table 3 Maximum, minimum, and mean values of the morphometric parameters for the Eyvanekey, Garmsar, and Semnan areas (fans, catchment basins, mountain fronts, and rivers)

Area	Fan	WLF	A_s	FA (km^2)	BA (km^2)	F_g	R (m)	FCI	FS	Vf	Smf	Fmf	Fd	AF %	T	Sl	BS	Bull	Viseras
Eyvanekey	Max	1.232	137	85.521	168.371	1.083	992	1.101	65.693	2.451	1.263	4.178	0.312	47.932	0.245	120.000	1.600	C	A
	Min	0.671	95	13.912	28.710	0.995	977	0.751	49.241	2.358				47.751	0.168	65.702	1.000	C	C
	Mean	0.952	116	49.717	98.541	1.039	984.5	0.926	57.467	2.405				47.842	0.207	92.851	1.300	C	C
Garmsar	Max	1.112	143	761.561	1092.702	49.671	28,831	2.639	72.443	4.646	1.442	7.485	1.124	77.558	0.791	1106.177	4.256	C&B	C
	Min	0.199	33	0.089	17.976	0.043	497	0.371	17.557	0.487	1.008	2.857	0.819	40.934	0.361	18.245	1.355	A&D	A&B
	Mean	0.618	78.317	29.707	141.295	7.34	3581.458	0.854	43.503	1.536	1.272	5.142	0.925	60.691	0.539	378.705	2.567	B&C	B&C
Semnan	Max	1.367	135	87.829	308.852	11.080	10,000	0.984	65.879	10.445	1.152	8.855	1.038	81.785	0.734	570.740	4.775	C	C
	Min	0.279	25	0.001	5.632	0.771	22	0.056	28.385	0.659	1.063	3.063	0.934	36.097	0.195	69.253	0.772	B&D	B
	Mean	0.641	71.524	14.261	90.356	3.599	3294.702	0.604	47.263	3.660	1.026	7.387	0.981	47.150	0.461	299.154	2.253	B&C	B&C

Also, the geological maps (1:250,000) of the Tehran (Haghipour et al. 1987) and Semnan (Aghanabati and Hamedi 1994) focus on the fault and fold structures that are located along the southern part of the Central and Eastern Alborz. Geometry and activity of some of these structures are poorly recognized (e.g., Sarasiab, Rameh, Kuh-e-Namakdan fault, and Lasjerd anticline). Also, alluvial fans as active deformation evidences are not mapped along the south edge of the Alborz Mountains. On the other hand, the blind structure activity and bedrock characteristic in the front zone of the Central and Eastern Alborz are unclear and need a more detailed investigation. We believe the data of fan morphology evidences, geoelectric profiles, and exploitation wells can improve information in this area. Based on morphometric indexes and subsurface data, distribution of active deformation in the Late Quaternary in the southern front of the Central and Eastern Alborz can be better identified.

The summary morphometric index data (Table 3) of fans, catchment basins, mountain fronts, and rivers suggest that the Late Quaternary compressional tectonic deformation in the Central and Eastern Alborz Mountains caused mostly shortening and uplifting of the crust. Based on the fan morphology evidences, we divided the Central Alborz into two areas according to Guest et al. (2006a): the Eyvanekey area in the west Central Alborz and the Garmsar area in the east Central Alborz. In the Central and Eastern Alborz, three-generation fans were formed. The first-generation fans are large and extended (e.g., Eyvanekey, Garmsar, Dehnamak, Lasjerd, Dehaghin, and Semnan). They are related to the high tectonic subsidence (Viseras and Fernandez 1994; Viseras et al. 2003) and uplifted deformation based on the exploitation well data. Moreover, intensive rainfall during the glacial age (Hosein-Khannazer 2015) increased the volume of sediment carried by regional rivers, so based on the Lasjerd exploitation well (15), mostly the first-generation fans are made from flood deposit, of the braided rivers. Except the west Central Alborz, the east Central Alborz, and Eastern Alborz, the second- and third-generation fans were formed. The Eyvanekey–Parchin reverse fault (Tchalenko 1974; Berberian 1974), Garmsar thrust fault (Berberian 1974), and Rameh and Semnan thrust faults (Nabavi 1976) are the active structures in the southern part of the Central and Eastern Alborz. Therefore, mostly fans are formed along these structures. Generally, the second-generation fans were formed over the first generation (e.g., Garmsar, Abdolabad, Sorkheh, Semnan). It means that the fans in the southern part of the anticlines (e.g., Lasjerd) in the Eastern Alborz are the result of the growing fold structures during the crust shortening. About 82% of fans are debris fans and formed along the minor faults (e.g., Jalilabad and Kuh-e-Namakdan faults) in front of the Garmsar and Semnan

faults. The result of the latest compressional deformation as a young mountain uplift and base level change are forming the third-generation fans, mainly in the east Central Alborz and Eastern Alborz. Based on the relatively complete cone shape in the west Central Alborz and the elongate shape in the east Central Alborz and Eastern Alborz, crust uplifting in the hanging wall of the Eyvanekey–Parchin reverse fault is less than the that of the Garmsar, Rameh, and Semnan thrust faults. Based on the uplifting hanging wall, all catchment basins are asymmetric and stretching. It means uplifting deformation is active in the Late Quaternary. The basin deformation in the east Central Alborz is more than the other parts. It is a direct relation between the alluvial fan area and catchment area in the first generation. In second-generation alluvial fans, in which generally the catchment area is bigger than the alluvial fan area, we supposed the catchment area is the same for two generations, so the second-generation fans are formed over the first based on the crust uplifting in the Alborz (Fig. 6). The crust shortening and uplifting in the Alborz Mountains is reflected to the fan slope and radius: the greater slope and radius of the Garmsar area in the east Central Alborz and then Semnan area in the Eastern Alborz and relative to the Eyvanekey area showed that the uplifted area in the east Central Alborz is higher than that in the Eastern Alborz. It is noticeable that evaporite mass movements (e.g., Sardareh, Rameh, and Lasjerd) in Late Quaternary affected the shape of alluvial fans. Around the evaporite mass, the alluvial fans are inclined (e.g., second-generation Lasjerd toward east and Garmsar fans to the east and Eyvanekey fan to the west). According to Stöcklin (1974), Allen et al. (2003), and Guest et al. (2006a), we believe that the northern part of the Central and Eastern Alborz accumulated with internal shortening. It is reflected on the catchment basin asymmetric shape and mountain front morphology indexes. So, more regional uplift was marked in the east Central Alborz. Also, Fmf and Fd in the Eastern Alborz (Table 3) suggested that fold active and evaporite mass uplifting in the Lasjerd to Sorkheh are caused by increasing multifaceted surface and raised the braided parts of the mountain front in the southern front of the Eastern Alborz zone. The evaporite mass uplifts are reflected to the Abdolabad and Garmsar fans extending in the east Central Alborz, too. Field evidences (Fig. 8), for instance the fracture of 4 m depth with N40E strike, to the south of the Sorkheh fan (Fig. 8m) are a result of the base level change in the Eastern Alborz or cutting the young deposits by the Sardareh evaporite mass (Fig. 8a) as reflected by crust uplifting in the Central Alborz. According to Guest et al. (2006a), McQuarrie et al. (2003), and Allen et al. (2004), fan morphology evidence indicated that in Late Quaternary, crustal shortening accommodated with

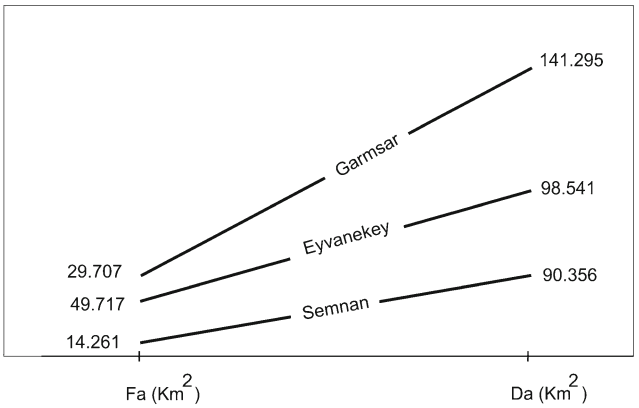

Fig. 7 Direct relationship between fan area and catchment basin area in the Eyvanekey, Garmsar, and Semnan areas

compressional deformation and uplifting in the east Central Alborz and Eastern Alborz. Although deformation rate is considerably decreased in the Eyvanekey area in the west of the Central Alborz, there are morphological evidences to indicate that this area is not completely inactive.

In addition, we suggest a fault zone in front of the east Central Alborz (Fig. 9a). This zone is between the Sarasiab sinistral fault system in the north and the Garmsar dextral fault system in the south (Fig. 9b). According to Guest et al. (2006a), these faults mostly show transpressional deformation.

Displacement of the direction of Hableh and Rameh rivers (3.57 km in the north and 1.33 km in the south) in the Garmsar and Dehnamak fans (Fig. 9b) is a result of this fault zone. According to Ballato et al. (2015), we believe that tectonic deformation is affected on the rivers in the Central Alborz. The fault zone (Fig. 9c) moved toward the east, and evaporite masses were exposed at the eastern part. It should be noted that these uplift and transpression deformations were linked to compression deformation (Fig. 9d). The changing orientation of Alborz structures from W–E to NE–SW, respectively, was probably the result of exposing these evaporite units (Fig. 9c). There is very little information on the Rameh and Lasjerd evaporite masses. Since these units are linearly exposing along the Rameh fault, it is likely might be a relationship between the fault direction and exposed evaporite units (Fig. 9c). Evaluation of the evaporite masses and salt sequence in the Garmsar Sardareh by Baikpour and Talbot (2012) showed that this salt unit was buried in the Garmsar basin and was exposed as the Garmsar salt nappe or the Garmsar salt glacier on the surface. This salt mass is allochthonous. They believed the ductile behavior of the salt sheets caused the aseismic strain of the area or to have less than recorded 3.5-magnitude earthquakes. In addition, the presence of these evaporite masses has been influenced by the reduction of wavelengths, surrounding folds. Its localization displacement has affected the behavior of faults, causing inversion in fault performance.

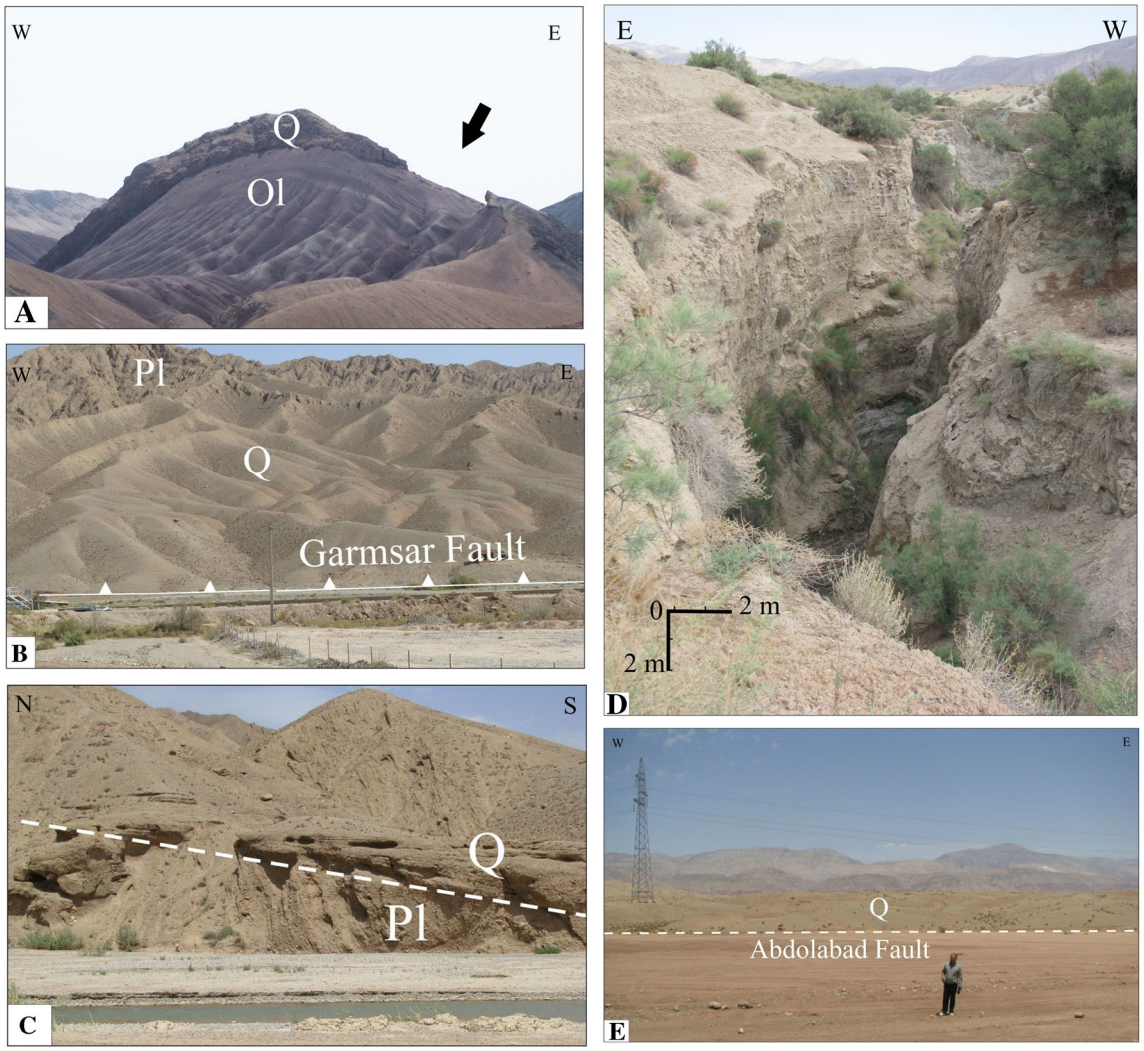

Fig. 8 **a** Evaporite unit uplift of Lower Red Formation and rupture of Quaternary deposits 5 km west of the Garmsar, view toward northeast. **b** Shrinkage and uplift of young Quaternary deposits in the Garmsar fault hanging wall in the Jalilabad region, view toward north. **c** Young Quaternary units with unconformities on Pleistocene tilted conglomerate unit along the Hableh River margin in the Garmsar, view toward east. **d** Base level changes in the Abdolabad riverbed showing deep gypsum valley with steep walls in smoothed bed, view toward south. **e** Linear uplift of Quaternary deposits along the Abdolabad fault in Dehnamak fan, view toward north. **f** Quaternary clay and sand fine sedimentary deposits + 10 m in thickness at the end of the Abdolabad fan in south the Abdolabad fault, view toward east. **g** Cross section of the sedimentary sequence in the Lasjerd fan with angled boulders among fine deposits showing heavy flooding of the Lasjerd River, view toward east. **h** Minor reverse fault and wall uplift of the Lasjerd River and formation of alluvial terraces, view toward northwest. **i** Uplift and formation of grooved water channels in ends of the Lasjerd fan, view toward south. **j** Evaporite mass uplift along the Rameh fault south of the Lasjerd fan that dam waters exit and rise in adjacent underground water level (proper land for agriculture), view toward south. **k** Alluvial terrace with medium-sized grain in the Dehaghin fan. Gypsum units form eastern uplift, view toward east. **l** Sorkheh northern anticline limb consisting of marl and limestone units of Qom Formation covered by Quaternary unconformity conglomerate, view toward northeast. **m** Changes in base level-forming groove of 4 m in depth at the southern end of the Sorkheh fan, view toward northwest. **n** Cross section of clay and sandstone sequence in Semnan River energy change. Base level changes in riverbed increased with uplift of old deposit outcrops, view toward east

We believe that the studied morphometric indexes of the adjacent fans to these evaporite masses provide valuable information on the movements of these evaporite masses. For example, the inclination of the second generation of the Garmsar fan to the east or the Eyvanekey fan to the west (Fig. 9c) could be the result of the Garmsar salt glacier movement or the shape of Lasjerd fans controlled by the Lasjerd evaporite mass (Fig. 2).

According to Hoth et al. (2007), we have shown evidences that strain or deformation in active structures has gradually transferred to the east Central Alborz front in the south (Fig. 2). The Abdolabad reverse fault parallel to the Garmsar–Rameh fault zone as a blind structure in the Central Iran shows continuation of Alborz dynamics. It is recognized according to geoelectric profiles (subsurface data) and the Safaeyeh fan (43) in the Garmsar area. The fan morphometry indexes (Table 2) such as the BS index

Fig. 8 (continued)

caused the sudden uplift along this fault. There are two possibilities existing in the Abdolabad fault: the first possibility, as an old structure which has been reactivated by the compressional tectonics, and the second one, as a new structure being formed under conditions of shortening deformation in the Late Quaternary.

Based on the study of Bull (1977), Dorn (1994), Roberts (1995), Calvache et al. (1997), Harvey (2002, 2005), Viseras et al. (2003), Gaetano et al. (2005), and Ballato et al. (2015), tectonic processes, base level changes, climate, and lithology are influenced in the formation and evolution of fans. In addition, we suggest the bedrock

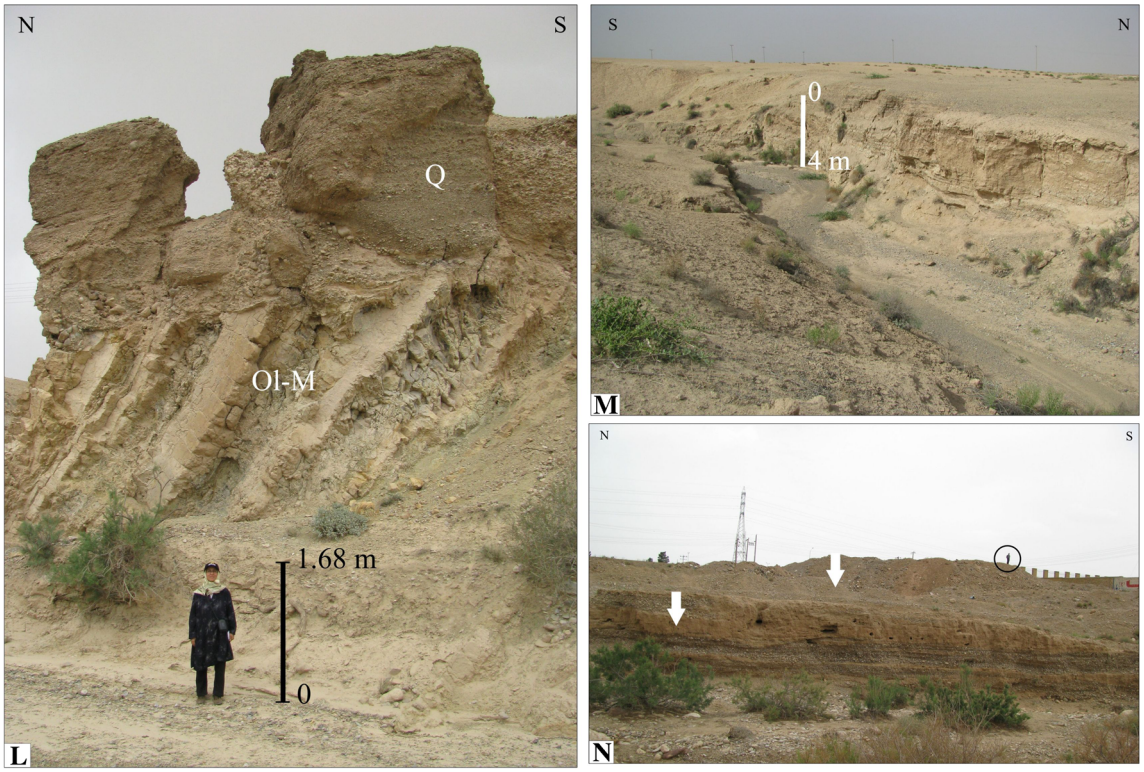

Fig. 8 (continued)

situation under the fans has a direct effect on the extended fan and its morphology.

Proposed fan models

According to Hosein-Khannazer (2015), during the Quaternary, epeirogeny is as active as orogeny but relatively weaker with regional and local activities. The results are uplifting and depressing of crustal blocks (horst and graben). As confirmed by Stöcklin (1968), these structural features have formed the southern front of the Eastern Alborz. Following Pinter et al. (2003) and Ballato et al. (2008), positive isostasy in the Alborz Mountains and negative isostasy in the Central Iran (in front of the Alborz Mountains) are active. Therefore, the result of the growth folds and uplift of the fault hanging wall is the thickening Alborz crust. Meanwhile, the response uplifting crust is subsiding in the vicinity blocks (Bloom 1967). We suggest this subsidence might have provided suitable places for forming alluvial and debris fans in the southern front of the Central and Eastern Alborz. According to Pedrami (1987), severe precipitation and flooding are characteristics of the Alborz glacial periods, suggesting, around the same time, the bedrock subsiding was necessary for providing enough space for forming and developing fans.

A summary evolution of the three generation fans in front of the Central and Eastern Alborz areas based on bedrock characteristic is shown in Fig. 10a and b.

In suggested models, the morphology of alluvial fans records important information about the bedrock topography in these areas. It is noticeable that in Late Quaternary, compressional tectonics and positive isostasy occurred with uplifting in the hanging wall and negative isostasy has occurred with subsidence in front of the Alborz Mountains.

The fan models of the Eyvanekey and Garmsar areas in front of the Central Alborz are shown in Fig. 10a. It should be mentioned that the bedrock in these areas is the same. So based on the bedrock topography, the first-generation and the second-generation alluvial fans formed to the southwest in Eyvanekey and continued southeast for Garmsar fans. As shown in this model, crust shortening and uplifting in the hanging wall of reverse faults parallel to the Garmsar fault caused the formation of the third-generation fans along these faults. On the other hand, the Sardareh evaporite mass movement along the Takht-e Rostam fault zone at the border between Eyvanekey and Garmsar areas caused tilting of the Eyvanekey fan to the west and Garmsar fan to the east. In addition, the Abardezh reverse fault in the southern Eyvanekey area controls this area fan extending to the south. The scarp fault in Fig. 10a shows that the uplift rate in the Garmsar area is relatively greater than that in the Eyvanekey

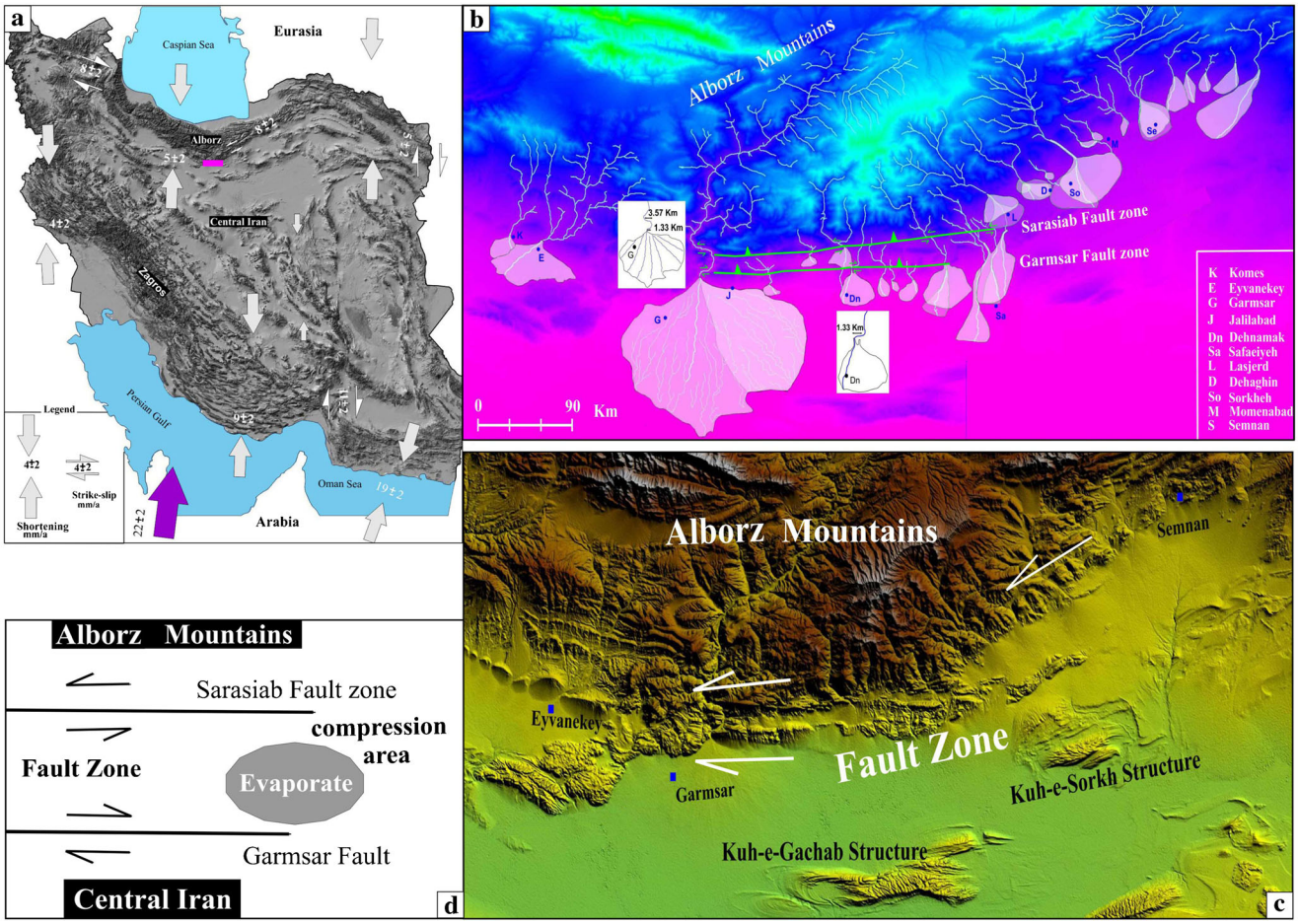

Fig. 9 **a** Location of the fault zone (red rectangle) in front of the Central Alborz Mountains, over simplified tectonic map with arrows showing sense of relative motion of shortening and shearing (Venant et al. 2004a). **b** Offset in the direction of the Hableh River in the Garmsar fan (G) and Rameh River in Dehnamak fan (Dn). They are showing the transpressional deformation on the Garmsar and Sarasiab fault zone. **c** Close up of the fault zone. **d** Schematic model of the fault zone and centralized evaporite mass in the east

area. One reason might be position of the Central Alborz Mountains to the general stress direction.

The fan model in the Semnan area in the Eastern Alborz is shown in Fig. 10b. Positive isostasy and crust shortening with compressional deformation in the Eastern Alborz occurred with uplifting in the hanging wall of thrust faults and uplifted the Rameh evaporite masses along the thrust faults and growth of the Lasjerd–Sorkheh folded structure.

These processes formed the second- and third-generation fans along the structures. The remarkable point is the

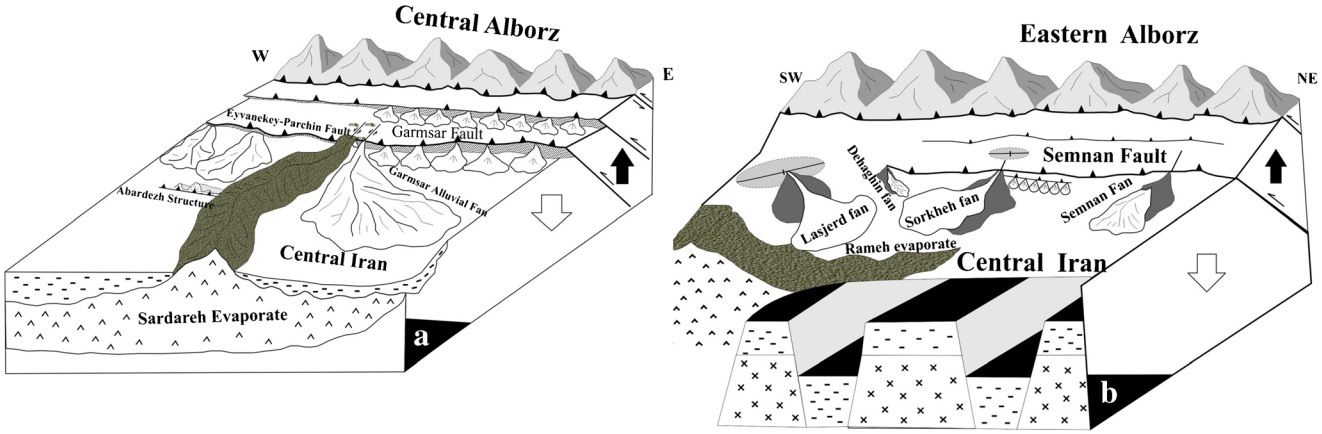

Fig. 10 Schematic models of alluvial fan development. **a** Eyvanekey and Garmsar. **b** Semnan

morphology of second-generation fan, such as the Lasjerd, Dehaghin, Sorkheh, and Semnan, which follows the topography of the bedrock. The brittle bedrock in the Semnan area and fracture along the minor faults (Sorkheh, Darjazin) formed horst and graben in the bedrock; thus, in this area, the second-generation fans trend toward grabens.

Therefore, the bedrock in the Garmsar and Eyvanekey areas is ductile, but in the Semnan area, it is brittle that reflected to the morphology of fans.

Conclusions

The southern front of the Central and Eastern Alborz Mountains in Eyvanekey, Garmsar, and Semnan is a noticeable area for recording significant data related to the late stages of the Arabia–Eurasia collision in Late Quaternary. The continent–continent collision caused the compressional deformation (e.g., Allen et al. 2004) and erosion (Morley et al. 2009) in this area. The reflect of continent convergence in the Alborz Mountains is accommodated with crust shortening and uplifting of the Alborz Mountains (Ballato et al. 2008), and transpressional deformation in the west Central Alborz (Guest et al. 2006a). In addition, positive isostasy (Ballato et al. 2008) and rising base level in the northern part of the Eyvanekey–Parchin, Garmsar, and Semnan reverse to thrust fault zone make a different topography along these faults (uplifted crust in the north and negative isostasy with subsided crust in the south). However, during the Quaternary, erosion and deposition of the sediment deposits caused the alluvial and debris fans to form in the southern front of the Central and Eastern Alborz. Analysis of 17 morphometric indexes for 131 fans in the Eyvanekey, Garmsar, and Semnan areas shows that the Alborz Mountains are affected by compressional tectonics. There is a relationship with uplifting and shortening crust. Positive isostasy and rising base level in the hanging wall of the thrust and reverse faults as well as the uplifting of folded structures and evaporite mass movement (Baikpour and Talbot 2012) are compensated for by negative isostasy and subsidence in the foot wall of the faults and southern front of the Central and Eastern Alborz. This phenomenon makes an efficient space for sediment deposits and formation of alluvial and debris fans along the reverse and thrust faults. The continuation of continent convergence and young uplifted crust in the Alborz Mountains are reflected to the shape and extended second- and third-generation fans over the first-generation fans. The third-generation fans reflect the young evolution of the east Central Alborz Mountains in this area. In this regard, the effect of the young pulse of the Pasadenian orogeny is often associated with base level changes. Fan morphology shows that the extended fan depends on various factors, like presence of rising structures such as the Abardezh structure in the south of the Eyvanekey area; evaporite mass like Rameh evaporite mass in the south of the Lasjerd fan prevents the growth of fan longitude, or the continuation of Sardareh evaporite mass movement is tied to the inclination of the Garmsar fan toward the east and the bedrock topography and activity.

The bedrock is not similar in these areas. Although in the Eyvanekey and Garmsar areas the bedrock is relatively ductile, the bedrock in the Semnan area is brittle. The subsided bedrock makes a suitable space for inclination of the fan toward it. The sudden trend change of the second-generation (Sorkheh) fan toward the west probably reflects the graben structural form on the bedrock. Crust uplifting is active in the Central and Eastern Alborz mostly in the east Central Alborz Mountains. It is indicated by the formation of valleys, deep grooves, and stepped terraces in the river traverse. River deposits form parallel layers, medium sorting, relatively good roundness, and medium-to-high thickness. The deposit facies are mostly fine to coarse grain.

Based on the morphology of alluvial fans, the young compression deformation in the east Central and Eastern Alborz is focused on the southern front of the Alborz toward Central Iran. For instance, formation of the Safaeyeh fan along the Abdolabad reverse fault (recommended in this research) in the east Central Alborz and formation of channels perpendicular to fans' extended direction (e.g., Sorkheh alluvial fan) in the Eastern Alborz mostly indicated the uplifting of crust and base level change in the east Central Alborz and Eastern Alborz, respectively. The morphology of Hableh and Rameh rivers which caused a fault zone with transpressional deformation is formed in the southern front of the east Central Alborz. In this fault zone, a local compressional deformation occurred in the eastern part.

We suggest fan morphology evidences give more detailed information related to the young compressional deformation in front of the mountains. Based on the evidences, we divided the southern front of the Central Alborz to the west (Guest et al. 2006a) and east. The uplifting crust in the east Central Alborz (Garmsar area) is relatively greater than that in the west Central Alborz (Eyvanekey area) and Eastern Alborz (Semnan area). Also, base level changes in the eastern Alborz are relatively higher than those in the east and west Central Alborz. Shortening and uplifting of crust, transpressional deformation in the fault zone, and formation or reactivity of the new reverse fault in the southern front of the east Central Alborz show compressional deformation is mostly accumulated in this part of the Central Alborz.

Fan evolution in the Central Alborz Mountains (Garmsar and Eyvanekey areas) follows a relatively simpler model than that in the Eastern Alborz Mountains (Semnan area) because of the brittle behavior of the bedrock in the Semnan area. Activation of the evaporite masses has effected fan morphology and must be considered in the analysis.

Moreover, the Quaternary climate (Pedrami 1987; Ballato et al. 2008) has definitely affected fan morphology and evolution in the study area.

Acknowledgments The author would like to thank Mr. Mohammad-Ebrahim Zakeri from Semnan Water Survey for his support of my research in several field surveys and the useful data provided. Special thanks to Professor Mohammad-Hasan Nabavi for reviewing the paper and for his fruitful discussion and suggestion. I am grateful to the anonymous reviewers for their thoughtful reviews and useful suggestions.

References

Agard P, Omrani J, Jolivet L, Mouthereau F (2005) Convergence history across Zagros (Iran): constraints from collisional and earlier deformation. Int J Earth Sci 94:401–419. https://doi.org/10.1007/s00531-005-0481-4

Aghanabati A, Hamedi AR (1994) Geological survey of Iran, Semnan sheet 1:250000

Alavi M (1996) Tectonostratigraphic synthesis and structural style of the Alborz Mountain system in Northern Iran. J Geodyn 21:1–33

Allen MB, Armstrong HA (2008) Arabia-Eurasia collision and the forcing of mid-Cenozoic global cooling. Palaeogeogr Palaeoclimatol Palaeoecol 265(1-2):52–58. https://doi.org/10.1016/j.palaeo.2008.04.021

Allen M, Ghassemi MR, Shahrabi M, Qoashi M (2003) Accommodation of late Cenozoic oblique shortening in the Alborz range, Northern Iran. J Struct Geol 25:659–672. https://doi.org/10.1016/S0191-8141(02)00064-0

Allen M, Jackson J, Walker R (2004) Late Cenozoic reorganization of the Arabia-Eurasia collision and the comparison of short-term and long term deformation rates. Tectonics 23:TC2008. https://doi.org/10.1029/2003TC001530

Ambraseys NN, Melville CP (1982) A history of the Persian earthquakes, Cambridge Earth Science Series. Cambridge University Press, London

Annells RN, Arthurton RS, Bazley RA, Davies RG (1975) Explanatory text of the Qazvin and Rasht quadrangles map, Geological Survey of Iran, E3 and E4, 94 P

Ashtari M, Hatzfeld D, Kamalian N (2005) Microseismicity in the region of Tehran. Tectonophysics 395:193–208

Assereto R (1963) The Paleozoic formation in Central Elburz (Iran), preliminary note. Riv Ital Paleontol Stratigr 69:503–543

Axen GJ, Lam PJ, Grove M, Stockli DF, Hassanzadeh J (2001) Exhumation of the west-central Alborz Mountains, Iran, Caspian subsidence, and collision-related tectonics. Geology 29:559–562. https://doi.org/10.1130/0091-7613(2001)029<0559:EOTWCA>2.0.CO;2

Azor A, Keller EA, Yeats RS (2002) Geomorphic indicators of active fold growth: South Mountain-Oak Ridge anticline, Ventura basin, Southern California. Geol Soc Am Bull 114:754–753

Bahrami S (2013) Tectonic controls on the morphometry of alluvial fans around Danehkhoshk anticline, Zagros, Iran. Geomorphology 180–181:217–230

Baikpour S, Talbot C (2012) The Garmsar salt nappe and seasonal inversions of surrounding faults imaged by SAR interferometry Northern Iran. Geol Soc Lond Spec Publ 363:563–578. https://doi.org/10.1144/SP363.28

Ballato P, Nowaczyk NR, Landgraf A, Strecker MR, Friedrich A, Tabatabaei SH (2008) Tectonic control on sedimentary facies pattern and sediment accumulation rates in the Miocene foreland basin of the southern Alborz Mountains, Northern Iran. Tectonics 27: TC6001. https://doi.org/10.1029/2008TC002278

Ballato P, Landgraf A, Strecker MR, Sudo M, Stockli DF, Friedrich A, Tabatabaei SH (2011) Arabia–Eurasia continental collision: insights from late Tertiary foreland-basin evolution in the Alborz Mountains, Northern Iran. Geol Soc Am Bull 123:106–131

Ballato P, Stockli DF, Ghassemi MR, Landgraf A, Strecker MR, Hassanzadeh J, Friedrich A, Tabatabaei SH (2013) Accommodation of transpressional strain in the Arabia-Eurasia collision zone: new constraints from (U-Th)/He thermochronology in the Alborz Mountains, North Iran. Tectonics 32:1–18. https://doi.org/10.1029/2012TC003159

Ballato P, Landgraf A, Schildgen TF, Stockli DF, Fox M, Ghassemie MR, Kirby E, Strecker MR (2015) The growth of a mountain belt forced by base-level fall: tectonics and surface processes during the evolution of the Alborz Mountains, N Iran. Earth Planet Sci Lett 425:204–218

Beaumont P (1972) Alluvial fans along the foothills of the Elburz Mountains, Iran. Palaeogeogr Palaeoclimatol Palaeoecol 12: 251–273

Benvenuti M (2003) Facies analysis and tectonic significance of lacustrine fan-deltaic successions in the Pliocene–Pleistocene Mugello Basin, Central Italy. Sediment Geol 157:197–234

Berberian M (1974) A brief geological description of North-Central Iran. In: Materials for the study of seismotectonics of Iran: North Central Iran. Geol. Surv. Iran, Rep. 29:127–138

Berberian M (19760 Contribution to the seismotectonics of Iran (part II), Geology Survey of Iran, Rep. No. 39, 58P

Berberian M (1983) The southern Caspian: a compressional depression floored by a trapped, modified oceanic crust. Can J Earth Sci 20: 163–183

Berberian M, King GCP (1981) Towards a paleogeography and tectonic evolution of Iran. Can J Earth Sci 18

Berberian M, Yeats RS (1999) Patterns of historical earthquake rupture in the Iranian plateau. Bull Seismol Soc Am 89:120–139

Berlin MM, Anderson RS (2007) Modeling of knickpoint retreat on the Roan Plateau, western Colorado. J Geophys Res 112:F03S06. https://doi.org/10.1029/2006JF000553

Blair TC (1987) Tectonic and hydrologic controls on cyclic alluvial fan, fluvial and lacustrine rift-basin sedimentation, Jurassic-lowermost Cretaceous Todos Santos Formation, Chiapas, Mexico. J Sediment Petrol 57:845–862

Blair TC, McPherson JG (1998) Recent debris-flow processes and resultant form and facies of the dolomite alluvial fan, Owens Valley, California. J Sediment Res 68:800–818

Blissenbach E (1954) Geology of alluvial fans in semi-arid regions. Geol Soc Am Bull 65:175–190

Bloom AL (1967) Pleistocene shorelines: a new test of isostasy. Geol Soc Am Bull 78:1477–1494

Bouzari S, Konon A, Koprianiuk M, Julapour AA (2013) Thin skinned tectonics in the Central Basin of the Iranian plateau in the Semnan area, Central Iran. J Asian Earth Sci 62:269–281

Bull WB (1964) Geomorphology of segmented alluvial fans in Western Fresno County, CA. USGS Prof Pap 352E:89–129

Bull WB (1977) The alluvial fan environment. Prog Phys Geogr 1:222–270

Bull WB (2007) Tectonic geomorphology of mountains. A new approach to paleoseismology. Blackwell, Oxford

Calvache ML, Viseras C, Fernandez J (1997) Controls on fan development — evidence from fan morphometry and sedimentology; Sierra Nevada, SE Spain. Geomorphology 21:69–84

Castillo M, Ferrari L, Salinas EM (2017) Knickpoint retreat and landscape evolution of the Amatlan de Canas half-graben (northern sector of Jalisco Block, western Mexico). J S Am Earth Sci 77:108–122

De Martini PM, Hessami K, Pantosti D, Addezio G, Alinaghi H, Ghafory-Ashtiani M (1998) A geologic contribution to the evaluation of the seismic potential of the Kahrizak fault (Tehran, Iran). Tectonophysics 278:178–199

DeCelles PG (2011) Foreland basin systems revisited: variations in response to tectonic settings. In: Busby C, Azor A (eds) Tectonics of sedimentary basins: recent advances. Wiley-Blackwell, Chichester, pp 405–426

Dellenbach J (1964) Contribution a letude geologique de la region situee a lest de Tehran (Iran). University Strasbourg 117 P

Djamour Y, Vernant P, Bayer R, Nankali HR, Ritz JF, Hinderer J, Hatam Y, Luck B, Le Moigne N, Sedighi M, Khorrami F (2010) GPS and gravity constraints on continental deformation in the Alborz Mountain range, Iran. Geophys J Int 183:1287–1301

Dorn RI (1994) The role of climatic change in alluvial fan development. In: Abrahams AD, Parsons AJ (eds) Geomorphology of desert environment. Chapman & Hall, London, pp 593–615

El Hamdouni R, Irigaray C, Fernández T, Chacón J, Keller EA (2008) Assessment of relative active tectonics, southwest border of the Sierra Nevada (southern Spain). Geomorphology 96:150–173

Francesca C, Ballato P, Alimohammadian H, Sabouri J, Mattei M (2014) Tectonic magnetic lineation and oroclinal bending of the Alborz range: implications on the Iran-southern Caspian geodynamics. AGU Tectonics 34:116–132. https://doi.org/10.1002/2014TC003626

Gaetano R, Muto F, Scarciglia F, Spina V, Critelli S (2005) Eustatic and tectonic control on Late Quaternary alluvial fans along the Tyrrhenian Sea coast of Calabria (South Italy). Quat Sci Rev 24:2101–2119

Gloppen TG, Steel R (1981) The deposits, internal structure and geometry in six alluvial fan-fan delta bodies (Devonian, Norway) — a study in the significance of bedding sequence in conglomerates. SEPM Spec Publ 31:49–69

Goswami PK, Pant CC, Pandey S (2009) Tectonic controls on the geomorphic evolution of alluvial fans in the Piedmont Zone of Ganga Plain, Uttarakhand, India. J Earth Syst Sci 118:245–259

Guest B, Axen GJ, Lam PS, Hassanzadeh J (2006a) Late Cenozoic shortening in the west-central Alborz Mountains, Northern Iran, by combined conjugate strike-slip and thin-skinned deformation. Geosphere 2:35–52. https://doi.org/10.1130/GES00019.1

Guest B, Stockli DF, Grove M, Axen GJ, Lam PS, Hassanzadeh J (2006b) Thermal histories from the Central Alborz Mountains, Northern Iran: implications for the spatial and temporal distribution of deformation in Northern Iran. Geol Soc Am Bull 118:1507–1521. https://doi.org/10.1130/B25819.1

Guest B, Guest A, Axen G (2007) Late Tertiary tectonic evolution of Northern Iran: a case for simple crustal folding. Glob Planet Chang 58:435–453. https://doi.org/10.1016/j.gloplacha.2007.02.014

Haghipour A, Taraz H, Vahdati Daneshmand F (1987) Geological quadrangle map of Iran, Tehran sheet, scale 1:250,000. Geological Survey of Iran, Tehran

Harvey AM (1988) Controls of alluvial fan development: the alluvial fans of the Sierra de Carrascoy, Murcia, Spain. Catena Suppl 13:123–137

Harvey AM (2002) The role of base-level change in the dissection of alluvial fans: case studies from Southeast Spain and Nevada. Geomorphology 45:67–87

Harvey AM (2005) Differential effects of base-level tectonic setting and climatic change on Quaternary alluvial fans in the northern Great Basin, Nevada, USA. J Geol Soc Lond 251:117–131

Harvey AM (2012) The coupling status of alluvial fans and debris cones: a review and synthesis. Earth Surf Process Landf 37:64–76

Heward AP (1978) Alluvial fan sequence and megasequence models, with examples from Westphalian D-Stephanian Bcoalfields, northern Spain. In: Miall AD (ed) Fluvial sedimentology. Mem. Can. Sot. Petrol. Geol. 5:669–702

Horton BK, Hassanzadeh J, Stockli DF, Axen GJ, Gillis RJ, Guest B, Amini A, Fakhari MD, Zamanzadeh SM, Grove M (2008) Detrital zircon provenance of Neoproterozoic to Cenozoic deposits in Iran: implications for chronostratigraphy and collision tectonics. Tectonophysics 451:97–122. https://doi.org/10.1016/j.tecto.2007.11.063

Hosein-Khannazer N (2015) Quaternary geology (Iranian alluvial). Geol. Surv. Iran., P:339 (in Farsi)

Hoth S, Hoffmann-Rothe A, Kukowski N (2007) Frontal accretion: an internal clock for bivergent wedge deformation and surface uplift. J Geophys Res 112:B06408. https://doi.org/10.1029/2006JB004357

Jackson JA, McKenzie DP (1984) Active tectonics of the Alpine-Himalayan belt between western Turkey and Pakistan, Geophys. J. R astr. Soc. 77

Jackson J, Priestly K, Allen M, Berberian M (2002) Active tectonics of the South Caspian Basin. Geophys J Int 148:214–245. https://doi.org/10.1046/j.1365-246X.2002.01588.x

Keller EA, Pinter N (1996) Active tectonics: earthquakes, uplift and landscape, New Jersey 338 PP

Koss JE, Ethridge FG, Schumm SA (1994) An experimental study of the effects of base-level change on fluvial, coastal plain and shelf systems. J Sediment Res 64:90–98

Lecce SA (1991) Influence of lithologic erodibility on alluvial fan area, western White Mountains, California and Nevada. Earth Surf Process Landf 16:11–18

Li YL, Yang JC, Tan L, Duan F (1999) Impact of tectonics on alluvial landforms in the Hexi Corridor, Northwest China. Geomorphology 28:299–308

Limber PW, Barnard PL (2018) Coastal knickpoints and the competition between fluvial and wave-driven erosion on rocky coastlines. Geomorphology 306:1–12

Mack GH, Leeder MR (1999) Climatic and tectonic controls on alluvial-fan and axial-fluvial sedimentation in the Plio-Pleistocene Palomas half graben, southern Rio Grande Rift. J Sediment Res 69(3):635–652

Masson F, Anvari M, Djamour Y, Walpersdorf A, Tavakoli F, Daignieres M, Nankali H, Van Gorp S (2007) Large-scale velocity field and strain tensor in Iran inferred from GPS measurements: new insight for the present-day deformation pattern within NE Iran. Geophys J Int 170:436–440. https://doi.org/10.1111/j.1365-246X.2007.03477.x

McQuarrie N, Stock JM, Verdel C, Wericke BP (2003) Cenozoic evolution of Neotethys and implications for the causes of plate motions. Geophys Res Lett 30(20):2036. https://doi.org/10.1029/2003GL017992

Moreno C, Romero-Segura MJ (1989) Abanicos aluviales actuales de pequeiia escala: aplicaci6n al estudio de materiales f6siles. In: Libro de Comunicaciones. XII Congreso Espaiiol de Sedimentologia, Madrid, pp 35–38

Morley CK, Kongwng B, Julapour AA, Abdolghafourian M, Hajian M, Waples D, Warren J, Otterdoom H, Srisuriyon K, Kazemi H (2009) Structural development of a major late Cenezoic basin and transpressional belt in Central Iran: the Central Basin in the Qom-Saveh area. Geoshere. 5(4):325–362. https://doi.org/10.1130/GES00223.1

Mouthereau F, Lacombe O, Vergés J (2012) Building the Zagros collisional orogen: timing, strain distribution and the dynamics of Arabia/Eurasia plate convergence. Tectonophysics 532(535):27–60

Mukerji AB (1976) The Chandigarh Dun alluvial fans: an analysis of the process form relationship. Panjab University, Chandigarh

Nabavi MH (1976) Semnan map, scale: 1: 250000. Geol. Surv. Iran

Nabavi MH (1998) Semnan map, scale: 1: 100000. Geol. Surv. Iran

Nemec W, Postma G (1993) Quaternary alluvial fans in southwestern Crete: sedimentation processes and geomorphic evolution. In: Marzo M, Puigdefàbregas C (eds) Alluvial sedimentation, vol 17. IAS Spec. Pubbl, pp 235–276

Pedrami M (1987) Quaternary stratigraphy of Iran. Geological Survey of Iran. Internal report, 551, 79 (55) (in farsi)

Pinter N, Sorlien CC, Scott A (2003) Fault-related fold growth and isostatic subsidence, California Channel Islands. Am J Sci 303: 300–318

Rezaeian M, Carter A, Hovius N, Allen MB (2012) Cenozoic exhumation history of the Alborz Mountains, Iran: new constraints from low-temperature chronometry. Tectonics 31:TC2004

Rieben EH (1966) Geological observations on alluvial deposits in Northern Iran, Geol. Surv. Iran, Rep. 9, 39 P

Ritz JF, Nazari H, Ghassemi A, Salamati R, Shafei A, Solaymani S, Vernant P (2006) Active transtension inside Central Alborz: a new insight into northern Iran–southern Caspian geodynamics. Geology 34:477–480. https://doi.org/10.1130/G22319.1

Roberts N (1995) Climatic forcing of alluvial fan regimes during the Late Quaternary in Konya basin, south central Turkey. In: Lewin J, Macklin MG, Woodward J (eds) Mediterranean Quaternary river environment. Balkema, Rotterdam, pp 205–217

Robustelli G, Muto F, Scarciglia F, Spina V (2002) Late Quaternary fan development and sea level change along the Tyrrhenian Sea coast of Calabria (southern Italy). Studi Geologici Camerti, Nuova Serie 2: 135–145

Rodríguez-Fenández LR, Heredia N, Seggiaro RE, González MA (1999) Estructura andina de la cordillera oriental en el área de la Quebrada de Humahuaca, provincia de Jujuy, NO de Argentina. Trab Geol 21: 321–332

Salfity JA, Brandán EM, Monaldi CR, Gallardo EF (1984) Tectónica compresiva cuaternaria en la Cordillera Oriental Argentina, Latitud de Tilcara (Jujuy). IX Congreso Geológico Argentino, Actas II, 427–434

Sancho C, Pena JL, Rivelli F, Rhodes E, Munoz A (2008) Geomorphological evolution of the Tilcara alluvial fan (Jujuy Province, NW Argentina): tectonic implications and palaeoenvironmental considerations. J S Am Earth Sci 26:68–77

Silva P, Harvey A, Zazo C, Goy JL (1992) Geomorphology, depositional style and morphometric relationships of Quaternary alluvial fans in the Guadalentin Depresion (Murcia, Southeast Spain). Z Geomorphol 36:325–341

Silva PG, Goj JL, Zazo C, Bardaji T (2003) Fault-generated mountain fronts in southeast Spain: geomorphologic assessment of tectonic and seismic activity, Geomorphology 50:203–225

Singh V, Tandon SK (2007) Evidences and consequences of tilting of two alluvial fans in the Pinjaur dun, northwestern Himalayan foothills. Quat Int 159:21–31

Srivastava P, Parkash B, Sehgal JL, Kumar S (1994) Role of neotectonics and climate in development of the Holocene geomorphology and soils of the Gangetic Plains between the Ramganga and Rapti rivers. Sediment Geol 94:129–151

Stampfli GM (1978) Etude geologique generale de l Elbourz oriental au sud de Gonbad-e-Qabus, Iran NE, These Geneve, 329 P

Stöcklin J (1968) Structural history and tectonics of Iran: a review: the American Association of Petroleum. Geol Bull 52:1229–1258

Stöcklin J (1974) Possible ancient continental margins in Iran. In: The geology of continental margins. Springer, pp 333–357

Storz-Peretz Y, Bowman D, Laronne JB, Svoray T (2011) Rapid incision of a small, coarse and steep fan-delta in response to base-level fall: the case of Nahal Qedem, the Dead Sea, Israel. Earth Surf Process Landf 36:467–480

Struth L, Castellanos DG, Muzas MV, Verges J (2019) Drainage network dynamics and knickpoint evolution in the Ebro and Duero basins: from endorheism to exorheism. Geomorphology 327:554–571

Tavakoli F (2007) Present-day deformation and kinematics of the Active faults observed by GPS in the Zagros and East of Iran (Ph.D. thesis). Universite Joseph Fourier, Grenoble I

Tchalenko JS (1974) Tectonic framework of the Tehran region, in material for the study of seismotectonics of Iran: north-central Iran. Geol Surv Iran, Rep 29:7–46

Van Hunan J, Allen MB (2011) Continental collision and slab breakoff: a comparison of 3-D numerical models with observations. Earth Planet Sci Lett 302:27–37

Vernant P, Nilforoushan F, Hatzfeld D, Abassi MR, Vigny C, Masson F, Nankali H, Martinod J, Ashtiani A, Bayer F, Chery J (2004a) Present-day crustal deformation and plate kinematics in the Middle East constrained by GPS measurements in Iran and northern Oman. Geophys J Int 157:381–398. https://doi.org/10.1111/j.1365-246X.2004.02222.x

Vernant P, Chery J, Bayer R, Djamour Y, Masson F, Nankali H, Ritz JF, Sedighi M, Tavakoli F (2004b) Deciphering oblique shortening of Central Alborz in Iran using geodetic data. Earth Planet Sci Lett 223: 177–185. https://doi.org/10.1016/j.epsl.2004.04.017

Vincent SJ, Morton AC, Carter A, Gibbs S, Barabadze TG (2007) Oligocene uplift of the western Greater Caucasus: an effect of initial Arabia–Eurasia collision. Terra Nova 19:160–166. https://doi.org/10.1111/j.1365-3121.2007.00731.x

Viseras C, Fernandez J (1994) Channel migration patterns and related sequences in some alluvial fan systems. Sediment Geol 88:201–217

Viseras C, Calvache ML, Soria JM, Fernández J (2003) Differential features of alluvial fans controlled by tectonic or eustatic accommodation space. Examples from the Betic Cordillera, Spain. Geomorphology 50:181–202

Westaway R (1994) Present-day kinematics of the Middle East and eastern Mediterranean. J Geophys Res 99:12071–12090

Whipple KX, Tucker GE (1999) Dynamics of the stream-power river incision model: implications for height limits of mountain ranges, landscape response timescales, and research needs. J Geophys Res 104:17661–17674

White K, Drake N, Millington A, Stokes S (1996) Constraining the timing of alluvial fan response to Late Quaternary climatic changes, southern Tunisia. Geomorphology 17:295–304

Zanchi A, Berra F, Mattei M, Ghassemi MR, Sabouri J (2006) Inversion tectonics in Central Alborz, Iran. J Struct Geol 28:2023–2037. https://doi.org/10.1016/j.jsg.2006.06.020